International Journal of Hydrogen Energy 134 (2025) 64–83

Contents lists available at ScienceDirect

International Journal of Hydrogen Energy

journal homepage: www.elsevier.com/locate/he

The potential of high-entropy alloys as catalyst materials in water-splitting application

Z.Y. Fan [a], M. Mucalo [b], J. Kennedy [c,d], F. Yang [a,*]

[a] Waikato Centre for Advanced Materials and Manufacturing, School of Engineering, University of Waikato, Hamilton, 3240, New Zealand
[b] School of Science, University of Waikato, Hamilton, 3240, New Zealand
[c] National Isotope Centre, GNS Science, PO Box 31312, Lower Hutt, 5010, New Zealand
[d] The MacDiarmid Institute for Advanced Materials and Nanotechnology, New Zealand

ARTICLE INFO

Keywords:
High-entropy alloys
Electrocatalytic water splitting
Hydrogen evolution reaction (HER)
Oxygen evolution reaction (OER)

ABSTRACT

High-entropy alloys (HEAs), which are characterized by the inclusion of five or more elements in nearly equiatomic configurations, have garnered increasing attention due to their distinct characteristics, including exceptional physical strength, superior corrosion resistance, outstanding microhardness, and long-lasting durability. The existence of multi-constituent elements in HEAs opens up unique possibilities for the development of compatible and innovative electrocatalytic active sites. Through careful selection of elements in terms of their combination and proportions, these electrocatalytic active sites demonstrate the potential of fine-tuning for numerous technical goals. Current studies have demonstrated the promising activities of HEAs into electrocatalytic areas. However, further enhancements in their activity explore interactions among component elements and require a deeper understanding of electrocatalytic active sites, as well as a deeper comprehension of the underlying electrocatalytic mechanisms. This review aims to provide an analysis of the four core characteristics (the high-entropy effect, the severe lattice distortion effect, the sluggish diffusion effect, and the cocktail effect) associated with electrocatalysts based on HEAs. Additionally, we delve into the various applications of HEAs related to electrochemical energy transformation reactions, which encompass both the hydrogen evolution and oxygen evolution reactions. The purpose of the review is to unravel the inherent complexities associated with electrocatalytic active sites, the interactions among component elements, and the mechanisms governing reactions in HEAs. Lastly, we highlight the urgent challenges and stress the importance of theoretical and experimental research, along with the underlying raison d'être of HEAs in electrocatalysis for supplying future energy needs. It is our expectation that this review will inspire additional investigation and advancement of HEAs in relevant electrocatalysis applications, particularly in the context of water splitting processes.

1. Introduction

The increasing global requirements for fossil fuels as populations increase globally, has given rise to profound climate and environmental challenges [1,2]. In response, there is a growing emphasis on researching eco-based technologies that aim for sustainable, eco-friendly energy sources [3,4]. A significant portion of recent investigation is dedicated to advancing electrochemical approaches related to water, which play a crucial role in efficiently harnessing and storing regenerative energy [5–7]. The effectiveness of these methods hinges on electrocatalytic water splitting, including the hydrogen evolution reaction (HER) and the oxygen evolution reaction (OER). Nevertheless, the widespread application of precious metals and their derivatives in these processes is hindered in terms of their relatively minor natural abundance, limited commercial availability, and huge economic cost [8–10]. Furthermore, operating instability in severe situations could cause some issues such as agglomeration, dissolution, and undesirable hazard tolerance based on precious electrocatalytic materials [11–13]. Hence, there is a pressing need to conceive and engineer affordable transition metal electrocatalysts that are outstanding in their effectiveness, naturally abundant, and economically viable, with the aim of comparing with or even surpassing the electrocatalytic activities of the known precious metal based rivals (see Table 1).

Alloys that are composed of both precious and non-precious metals

* Corresponding author.
E-mail address: fei.yang@waikato.ac.nz (F. Yang).

https://doi.org/10.1016/j.ijhydene.2025.04.477
Received 27 January 2025; Received in revised form 28 March 2025; Accepted 27 April 2025
Available online 4 May 2025

form an important category of uniform electrocatalysts as they demonstrate excellent durability, various and beneficial selectivities, as well as enhanced electrocatalytic performances compared to that exhibited by materials composed of only single metals. This improvement could be ascribed to the synergistic effects and alterations in *d*-band centre positions resulting from the alloying process [14–17]. Alloying introduces various changes in the thermal and physical features of the metal compositions, with electrocatalytic efficacy primarily influenced collectively by strain, ensemble, and ligand effects [18,19]. The classification of these alloys is associated with the number of compositions, ranging from binary and ternary to quaternary and high-entropy alloys. Despite their potential, the development of traditional alloy electrocatalysts faces diverse significant challenges. This is because the phase diagrams of bimetallic alloys often exhibit substantial immiscibility gaps which restricts the adjustment of component mole ratios and well-optimised electrocatalytic performance [20–22]. Additionally, the inadequate corrosion resistance of the majority of transition metals presents massive barriers for actual realisation of practical use under both alkaline and acidic conditions [23,24].

High-entropy alloys (HEAs) typically consist of five or more elements associated with varying atomic ratios, exhibiting an unsorted nanostructure that imparts superior properties compared to conventional alloys [25–27]. Primarily, HEAs demonstrate exceptional physical and thermal attributes, including excellent durability, heightened strength, and considerable corrosion resistance, which enables them to be highly useful as functional materials [28–33]. The distinctive features of HEAs can be attributed to four core effects: the high-entropy effect, the severe lattice distortion effect, the sluggish diffusion effect, and the cocktail effect [34]. The high-entropy effect is central to HEAs, resulting from the inclusion of multiple near-equimolar compositions. This results in the formation of a simple solid solution (SS) phase such as body-centred cubic (BCC), face-centred cubic (FCC), and hexagonal close-packed (HCP) phases instead of intermetallic components [27,35,36]. This enhances microstructural stability and configurational entropy [37]. The presence of numerous primary elements triggers sluggish diffusion rates, facilitating the straightforward formation of nanoprecipitates. This property is particularly crucial for applications in energy preservation and transformation [38–40]. In addition, the lattice distortion in HEAs contributes to the creation of strains and defects, known to significantly boost the electrocatalytic performance of alloys. Consequently, this aspect makes high-entropy alloys promising candidates for electrocatalysis applications. The cocktail effect of high-entropy alloys highlights their potential as electrocatalysts, where the synergistic interactions among the various compositional elements led to favourable activities as sustainable materials in electrochemical applications. This is ascribed to their diverse components, stabilized nature, and superior electrocatalytic capabilities of HEAs, positioning them as promising materials for future applications in electrocatalysis [41,42].

As stated earlier it is the intention of this review to provide a comprehensive overview of recent advances in the electrocatalytic applications of high-entropy alloys. We will start by delving into the four core characteristics defining these alloys. Subsequently, an exposition of the mechanistic understandings gleaned and the reported electrocatalytic activities of the recent breakthroughs regarding HEAs electrocatalysis will be covered. These will encompass both the HER and OER processes. Our discussion involves the impact of the element synergy inherent and multiple active site nature in HEAs on electrocatalytic performance, elucidated via both experimental evidence and through

Table 1
Summary of electrochemical activities for HEAs and other state-of-the-art catalysts under diverse conditions.

Reaction type	Electrode material	Electrocatalyst structure	Electrolyte	Activity	Stability	Ref.
HER	FeCoPdIrPt@GO	Nanoparticles	1.0 M KOH	η_{10} = 42 mV	150 h at 10 mA cm^{-2}	[65]
	PdFeCoNiCu NPs	Nanoparticles	1.0 M KOH	η_{10} = 18 mV	15 h at 10 mA cm^{-2}	[67]
	FeCoNiMnRu/CNFs	Nanoparticles	1.0 M KOH	η_{100} = 71 mV	600 h at 1.0 A cm^{-2}	[68]
	CuAlNiMoFe	Porous bulk	1.0 M KOH	η_{100} = ~56 mV	200 h at 50 mA cm^{-2}	[70]
	NiFeCoCuTi	Porous bulk	1.0 M KOH	η_{1000} = ~134 mV	240 h at 50 mA cm^{-2}	[71]
	FeCoNiCuMn HEA/CNF	Nanoparticles	1.0 M KOH	η_{100} = 281 mV	20 h at 170 mA cm^{-2}	[110]
	RuRhPdAgOsIrPtAu NPs	Nanoparticles	0.15 M H_2SO_4	η_{10} = ~60 mV	–	[111]
	PdMoGaInNi	Nanosheets	0.5 M H_2SO_4	η_{10} = 13 mV	12 h at 10 mA cm^{-2}	[112]
	NiFeMoCoCr	Bulk	0.5 M H_2SO_4	η_{100} = 281 mV	~8 h at 100 mA cm^{-2}	[113]
			1.0 M KOH	η_{10} = 172 mV	–	
	FeCoNiMnRu HEA/CNF	Nanoparticles	1.0 M KOH	η_{10} = 37 mV	36 h at 100 mA cm^{-2}	[114]
	RuNi/$ZrNiN_x$	Bulk	1.0 M KOH	η_{2000} = 392.8 mV	1000 h at 500 mA cm^{-2}	[115]
	$Co(OH)_2$@$Co_2Mo_3O_8$	Bulk	1.0 M KOH	η_{10} = 85 mV	30 d at 100 mA cm^{-2}	[116]
	NiCoFeMnCrP	Nanoparticles	1.0 M KOH	η_{10} = 220 mV	24 h at 220 mA cm^{-2}	[117]
	(MoWVNbTa)C	Nanoparticles	0.5 M H_2SO_4	η_{10} = 156 mV	48 h at 225 mA cm^{-2}	[118]
	$(Fe_{0.27}Ni_{0.35}Co_{0.24}Cr_{0.10}Mn_{0.04})_2O_{3-\delta}$	Nanoparticles	1.0 M KOH	η_{10} = 60 mV	20 h at 10 mA cm^{-2}	[119]
	CoZnCdCuMnS@CF	Nanoarrays	1.0 M KOH	η_{10} = 173 mV	70 h at 10 mA cm^{-2}	[120]
OER	AlNiCoIrMo	Porous bulk	0.5 M H_2SO_4	η_{10} = 233 mV	7000 cycles	[98]
	FeCoNiIrRu/CNFs	Nanoparticles	0.5 M H_2SO_4	η_{10} = 241 mV	14 h at 10 mA cm^{-2}	[100]
	FeCoNiRu	Nanoparticles	1.0 M KOH	η_{10} = 243 mV	40 h at 10 mA cm^{-2}	[101]
	np-AlNiFeCoMo	Porous bulk	1.0 M KOH	η_{10} = ~243 mV	40 h at 10/20 mA cm^{-2}	[104]
	MnFeCoNiCu@NPC/CC	Nanoparticles	1.0 M KOH	η_{10} = 263 mV	24 h at 10 mA cm^{-2}	[106]
	FeNiMnCrCu	Bulk	1.0 M NaOH	η_{40} = 466 mV	10 h at 438 mV	[107]
	CrMnFeCoNi HEA/NF	Bulk	1.0 M NaOH	η_{10} = ~280 mV	300 h at 10 mA cm^{-2} + 60 h at 100 mA cm^{-2}	[109]
	FeCoNiMnW/CP	Bulk	0.5 M H_2SO_4	η_{10} = 512 mV	60 h at 50 mA cm^{-2}	[121]
	FeNiMoCrAl	Thin film	1.0 M KOH	η_{10} = 220 mV	50 h at 10 mA cm^{-2} + 50 h at 100 mA cm^{-2}	[122]
	CoCrFeNiMo	Porous bulk	1.0 M KOH	η_{10} = 440 mV	24 h at 100 mA cm^{-2}	[123]
	CoFeGaNiZn	Nanoparticles	1.0 M KOH	η_{10} = 370 mV	10 h at 10 mA cm^{-2}	[124]
	$Ni_{0.24}Co_{0.23}Cu_{0.24}Fe_{0.15}Cr_{0.14}$/CP	Nanoparticles	1.0 M KOH	η_{10} = 232 mV	50 h at 10 mA cm^{-2}	[125]
	MoZnFeCoNi	Porous bulk	1.0 M KOH	η_{10} = 221 mV	1500 h at 100 mA cm^{-2}	[126]
	$Ni_xFe_{1-x}S_2$	Bulk	1.0 M KOH	η_{10} = 120 mV	550 h at 1.0 A cm^{-2}	[127]
	Zn–NiOOH	Subnanowires	1.0 M KOH	η_{10} = 179 mV	800 h at 200 mA cm^{-2}	[128]
	NiCoFeMnInS	Nanocrystals	1.0 M KOH	η_{10} = 313 mV	2200 cycles	[129]
	$(CuNiFeCoZnMnMg)F_2$	Bulk	1.0 M KOH	η_{10} = 292 mV	6 h at 10 mA cm^{-2} + 6 h at 50 mA cm^{-2}	[130]
	CoFeCuMn–CNO	Porousnanocube	1.0 M KOH	η_{10} = 328 mV	72 h at 400 mV	[131]
	$(Y_{0.2}Ho_{0.2}Dy_{0.2}Gd_{0.2}Pr_{0.2})_2Ru_2O_7$	Bulk	0.5 M H_2SO_4	η_{10} = 200 mV	50 h at 10 mA cm^{-2}	[132]

theoretical simulations. Last but not least, we highlight the persistent issues and the future potential in the evolution of HEA electrocatalysts for energy storage and electrochemical transformations. The review, it is hoped, will serve readers working in this area as an inspiration for the field which will aid in the selection of elements and assist the design strategy of HEAs tailored for particular reactions. Furthermore, it provides insights into the optimization of HEA compositions to amplify their intrinsic performance.

2. Properties of high-entropy alloys

The significance of high-entropy alloys lies in their strong influence on microstructure and properties, as highlighted by the four fundamental effects introduced in a 2006 publication [34]. These effects encompass the high-entropy effect, governing thermodynamic aspects, the sluggish diffusion effect dictating kinetic phenomena, the severe lattice distortion effect (shaping the structural characteristics), and the cocktail effect which underpin the diverse array of properties. Fig. 1 illustrates the interplay of these four core effects, so elucidating their impact on the field of physical metallurgy in the context of HEAs [43,44]. The consideration of high-entropy effects is crucial when assessing the free energies of various states in order to establish both the microstructure and equilibrium structure, as well as to comprehend the driving forces leading to the state of equilibrium. Additionally, the presence of sluggish diffusion has a significant impact on the rates of growth and nucleation during phase transformations. Severe lattice distortion has a profound impact on both the mechanical and physical properties of materials. This distortion significantly influences characteristics such as strength, sensitivity to strain rate, and ductility, while also exerting a notable effect on properties like electrical resistivity and magnetism. Consequently, these alterations disrupt the established interconnections among these properties, microstructure, and applications. Furthermore, this lattice distortion exerts its influence on critical thermodynamic and kinetic factors including strain energy, diffusion, mixing enthalpy, recovery tendencies, and lattice potential energy. The "cocktail effect" represents the holistic influence on material properties, encompassing a combination of factors including composition, structure, and microstructure. In addition to adhering to the mixture rule dictated by composition, this effect is amplified by the interplay between constituent elements, lattice distortions, and phase distribution, which collectively contribute an excess amount to each property. While it is worth noting that external variables like temperature, stress, and strain rate encountered during processing or field applications can also impact the microstructure, crystal structure, and properties, it remains that these four fundamental effects still maintain firmly at the core.

3. Electrocatalytic applications of high-entropy alloys (HEAs)

HEAs possess distinctive physical and chemical characteristics that render them appealing for use in electrocatalytic applications. The diverse composition within HEAs facilitates the customization to adjust surface nanostructure, creating electrocatalytic reaction sites that influences the chemical adsorption energy of intermediates and reactants. This, in turn, leads to enhanced electrocatalytic activities. Furthermore, the enduring durability conferred by the sluggish diffusion effect and high-entropy effect within HEAs makes them well-suited for various applications. This section delves into the potential uses for HEAs in electrocatalytic water splitting process including the hydrogen evolution reaction (HER) and oxygen evolution reaction (OER). The discussion aims to provide design strategies and to highlight recent advancements in water-splitting research for HEAs.

3.1. High-entropy alloys (HEAs) for the hydrogen evolution reaction (HER)

3.1.1. Introduction to the HER

The HER concerns two-electron transfer processes taking place above the surface of electrocatalysts, which can manifest via the Volmer-Tafel or Volmer-Heyrovsky mechanisms [47,48]. The binding affinity of catalytic reaction species holds pivotal importance in dictating electrocatalytic performances of the HER process. The Tafel slope, as determined via linear sweep voltammetry (LSV), determines the potential speed-controlling step [49,50]. The reaction pathway of the HER process exhibits variability determined by the pH value of the solution (Fig. 2) [51]. Under acidic conditions, the process begins with the formation of H* intermediates from proton donation by the acidic aqueous electrolyte. The prevalence of hydronium ions (H_3O^+), substantially enhances the rate of proton transfer, thereby fostering rapid electrocatalytic kinetics [52,53]. Hence, the Gibbs free energy associated with hydrogen adsorption (ΔG_{H^*}) emerges as a crucial criterion governing the

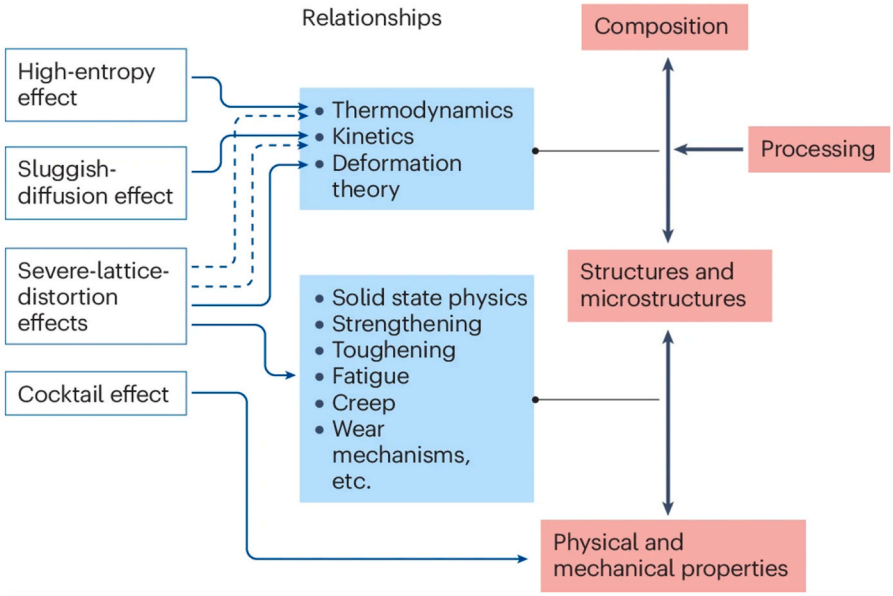

Fig. 1. The scheme of physical metallurgy and the influence from the four core effects. Solid arrows show that the effect is direct while dashed arrows represent that the effect is an indirect one [45,46]. Copyright 2024 Nature Publishing Group.

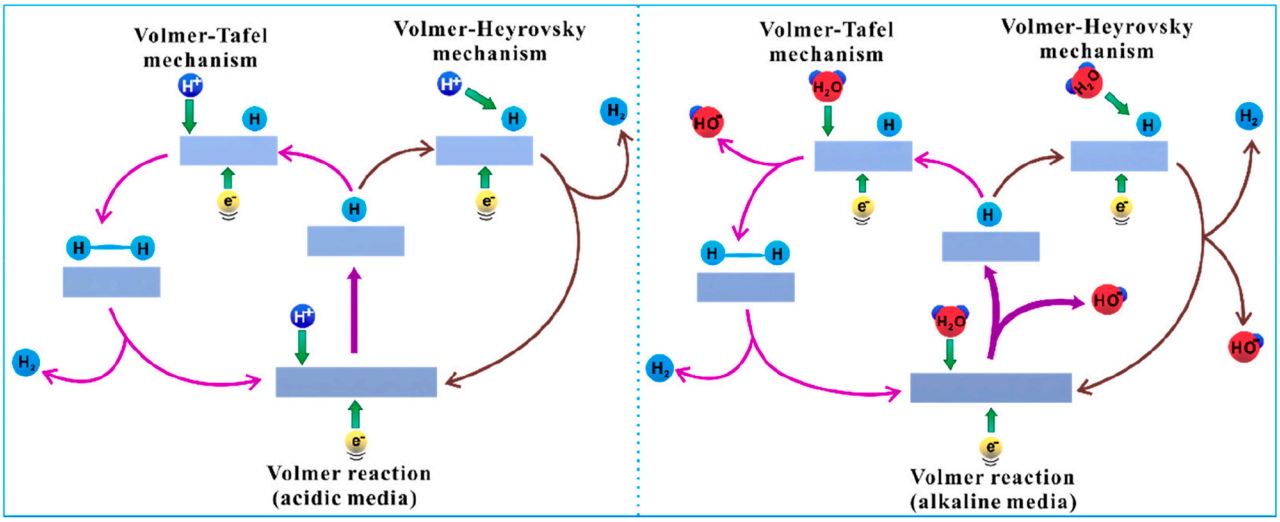

Fig. 2. Mechanism of hydrogen evolution reaction on the surface of an electrode in acidic (left) and alkaline (right) solutions [51]. Copyright 2020 American Chemical Society.

efficacy of reaction of the HER process in an acidic medium [54]. Conversely, in alkaline electrolytes, HER progresses via the Volmer stage, which involves the dissociation of water, the generation of active hydrogen intermediates, as well as subsequent Tafel or Heyrovsky reorganization stage [55,56]. Contributors such as H* intermediates adsorption on the electrocatalyst surface, kinetic obstacles during water dissociation, and the aggregation of OH* intermediate adsorption predominantly dictate the HER performance under alkaline conditions. The relevant reaction equations are listed below:

Overall reaction:

$$2H_2O \rightarrow 2H_2 + O_2 \quad (1a)$$

Cathode reaction under acidic situations:

$$2H^+ + 2e^- \rightarrow H_2 \quad (2)$$

HER mechanism under acidic situations:

$$\text{Volmer step}: H_3O^+ + e^- \rightarrow H_{ad} + H_2O \quad (3)$$

$$\text{Heyrovsky step}: H_3O^+ + e^- + H_{ad} \rightarrow H_2O + H_{2(g)} \quad (4)$$

$$\text{Tafel step}: 2H_{ad} \rightarrow H_{2(g)} \quad (5a)$$

Cathode reaction under alkaline situations:

$$2H_2O + 2e^- \rightarrow H_2 + 2OH^- \quad (6)$$

HER mechanism under alkaline situations:

$$\text{Volmer step}: H_2O + e^- \rightarrow H_{ad} + OH^- \quad (7)$$

$$\text{Heyrovsky step}: H_2O + e^- + H_{ad} \rightarrow OH^- + H_{2(g)} \quad (8)$$

$$\text{Tafel step}: 2H_{ad} \rightarrow H_{2(g)} \quad (5b)$$

While electrocatalysts based on Pt exhibit superior efficiency in the HER process, the prohibitive expense of Pt poses sustainability and economic viability challenges [57]. A promising technique lies in the doping of noble metal alloys comprising Ir, Pd, Ru, and Pt in conjunction with non-precious metals [58]. The advent of HEAs provides a prospective and facile pathway to crafting alloy electrocatalysts based on noble metals featuring reduced proportions of the precious elements. This approach holds potential for facilitating application effectiveness, curtailing costs, and concurrently upholding, if not enhancing, the superior electrocatalytic durability and activity characteristics compared to just using the pure Pt catalysts alone.

3.1.2. Design strategy for better HER electrocatalysts

The HER process involves both proton (H^+) and hydroxide (OH^-) intermediates, and with the aim of enhancing electrocatalytic performance, can be accomplished by tailoring catalytic active sites on substrates to favour one species over the other. Improving the thermodynamic properties of the reaction is achievable via lowering the activation energies for hydrolysis, and improving the catalysis kinetics requires a favouring of the particular adsorption process of the H atom on the surface of electrodes. Conversely, in the hydrolysis reaction, OH adsorption can also compete strongly with the adsorption of H* at an individual electrocatalytic active site, thereby diminishing the release of H_2 [48,59]. Moreover, it is challenging to establish or control the balance of adsorption of H*, OH*, as well as other reaction species at an individual electrocatalytic active site. To address the competition between H* and OH* species at electrocatalytic active sites in the HER, some strategies have been suggested to design these active sites with distinct functionalities [60–62]. These strategies can modify single catalytic species and regulate the *d*-band centre of the H* binding active site via optimizing multi-compositional metal choices. Incorporating precious metals into non-precious metals has already been demonstrated to strengthen HER activity. The fundamental technique for enhancing the performance of HER electrocatalysts involves achieving an optimal balance of water dissociation and hydrogen adsorption processes on the surfaces of the electrocatalysts [63,64]. HEAs, characterized by tunable constitutions with multiple components, provide a promising pathway which could be broadly applied with numerous metal elements under specific ratios to modulate reaction species adsorption on electrocatalytic active sites, thereby enhancing electrocatalytic performance while decreasing cost.

3.1.3. Precious-metal based HEAs for the HER

The incorporation of Pt alongside other metal elements into HEAs gives enhanced electrocatalytic efficacy for the HER process in terms of the synergistic interplay amongst the multiple metal constituents. This methodology provides for the application of minimal quantities of precious Pt but at the same time upholding or even elevating electrocatalytic durability and efficiency of the electrocatalyst. This hence leads to greater effectiveness and reduced expense. Gao and colleagues have illustrated the promise of nano-structural HEAs based on Pt as very useful electrocatalysts during the HER process [65]. Through the fast-moving bed pyrolysis (FMBP) process, they were able to make a series of multi-compositional HEAs for the purpose of investigating the electrocatalytic behaviours of various HEAs (Fig. 3a). Specifically in

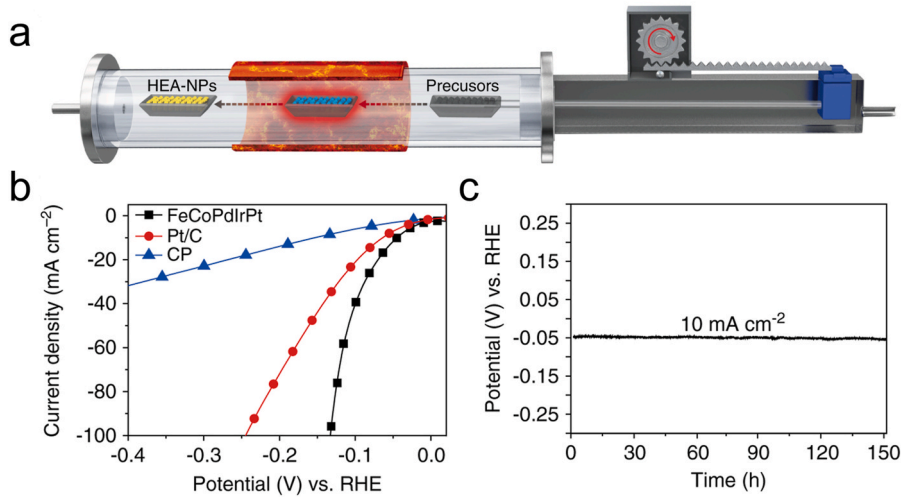

Fig. 3. (a) Schematic diagram of the FMBP experimental setup for synthesis of HEA-NPs. (b) The activities toward HER of the prepared FeCoPdIrPt, Pt/C, and pure CP through the FMBP strategy allows electrodes. Linear sweep voltammetry (LSV) curves were conducted to evaluate the activity toward HER at a scan rate of 5 mV s^{-1} with *iR* correction. (c) Chronopotentiometry curve for FeCoPdIrPt. Reprinted with permission from Ref. [65]. N.B. In this copyrighted image, it should be noted that "precursors" has been misspelt and is written as "precusors". Copyright 2020 Nature Publishing Group.

their systems studied, the quinary FeCoPdIrPt HEA nanoparticles (HEA-NPs) displayed very promising activities with a mass activity of 26 times greater than that observed industrial Pt/C, as well as very good catalyst stability lasting longer than 150 h (Fig. 3b and c). This exemplifies the advantages emanating from the component synergistic interaction within HEAs, highlighting their promise in advancing electrocatalytic technologies. The investigation also revealed the potential for finely tuning the ΔG_{H^*} of HEAs through the incorporation of Ir and Co metals, while Pd played a pivotal role in influencing the hydrogen binding energy (HBE) above its surface. Moreover, the presence of Fe, Pd and Co metals was observed to diminish the anti-bonding energy of elemental Pt, consequently promoting the desorption reaction of H* intermediates and the subsequent production of H_2. Furthermore, Feng et al. fabricated minimal sub-2 nm FeCoNiRhPt HEA nanoparticles and

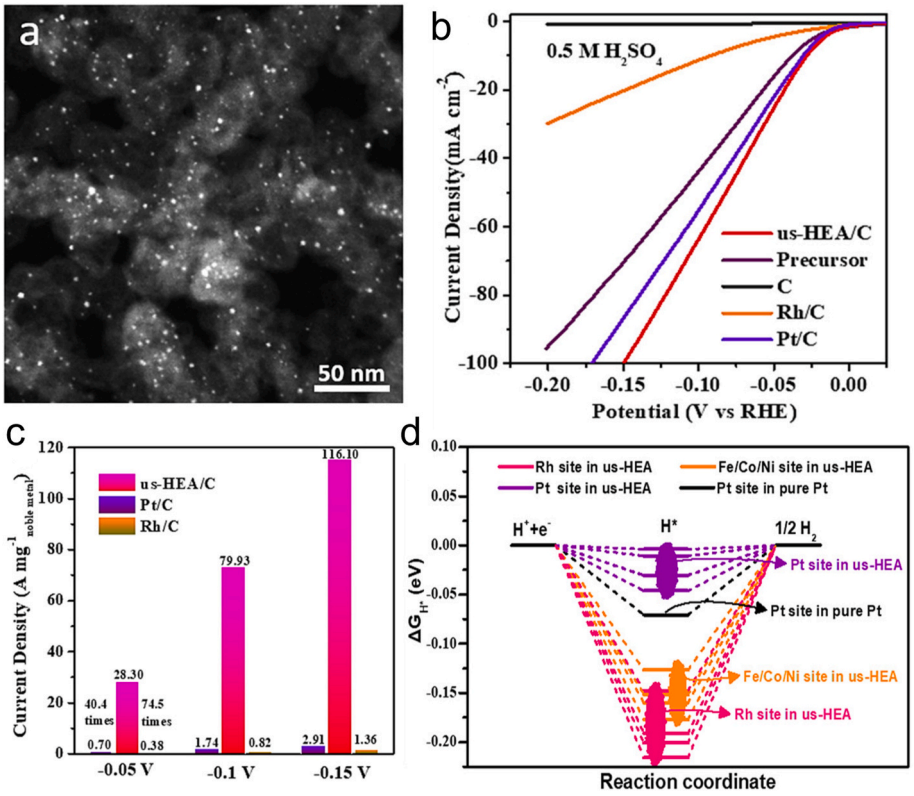

Fig. 4. (a) Representative high-angle annular dark-field scanning transmission electron microscopy (HAADF-STEM) image of ultrasmall (around 1.68 nm) FeCoNiRhPt ultra small high-entropy alloy (us-HEA) nanoparticles (NPs). (b) HER polarization curves of us-HEA/C, the precursor, Ketjen-black carbon (C), commercial Rh/C, and commercial Pt/C electrocatalysts in 0.5 M H_2SO_4 solution. (c) Quantitative comparisons of the mass activities of us-HEA/C, commercial Rh/C, and commercial Pt/C at different potentials. (d) Calculated hydrogen-adsorption free energy (ΔG_{H^*}) profiles for three representative sites on the us-HEA (111) surface and Pt site on pure Pt (111) surface at monolayer hydrogen coverage ($\theta_{H^*} = 1$). Reprinted with permission from Ref. [66]. Copyright 2021 American Chemical Society.

also suggested the remarkable electrocatalytic efficiency in the HER process under 0.5 M H_2SO_4 solution (Fig. 4a–b) [66]. These fabricated nanoparticles exhibited an exceptionally superior mass activity with the value of around 28.2 A mg^{-1} under −0.05 V, surpassing the performance of industrial Pt/C electrocatalysts by 40.4 times (Fig. 4c). Experimental observations showed that Pt and Rh served as the principal electrocatalytic active sites, with Co, Ni, and Fe productively optimizing the electronic configurations of Rh and Pt elements, ultimately increasing the system's overall entropy (Fig. 4d). These investigations underscore the potential of HEA nanoparticles to be effective and efficient HER electrocatalysts, which leverage the synergistic interplay between the diverse constituents.

Likewise, the nanoparticle HEAs based on Pt are garnering research attention for their remarkable catalytic abilities in the HER process. A recent study demonstrated that PdFeCoNiCu HEA nanoparticles fabricated via a one-pot method could reveal the relevant reaction mechanisms associated with the exceptional HER activities (Fig. 5a) [67]. Notably, surface-activated bonding and anti-bonding orbitals near the Fermi level predominantly cluster around the Ni and Co sites, suggesting their significance as electrocatalytic active sites of relevance for the main stage of water splitting during the HER process. The Projected Density of States (PDOS) analysis reveals charge-abundant characteristics at the Cu and Pd sites (Fig. 5b), whereas superior electrical performances are observed at the Co and Ni sites. Additionally, Pd facilitates proton adsorption activity crucial for the HER process, while Co majorly functions as the centre for an electron sink, enabling water adsorption and subsequent dissociation (Fig. 5c–d). The proximity of Ni contributes to stabilizing hydroxide ions (OH^-) in water splitting and aids in proton capture at Pd positions, promoting hydrogen gas production. Fe plays a significant role in compensating for charge deficits into adjacent Co sites, ensuring sustained excellent performances throughout the HER process. Lastly, the charge-abundant nature of Cu facilitates efficient electron delivery among the diverse transition metal active sites. The exceptional HER activity displayed is ascribed to the finely tuned electronic structures and synergistic relationships in quinary HEA materials, highlighting the significance of their favourable interplay.

Research findings indicate that HEAs based on elemental Ru have demonstrated good efficiency in the HER process. Hao et al.'s investigation revealed that within FeCoNiMnRu nanoparticles, Co sites exhibit the highest activity for water splitting with the minimum energy barrier recorded at 0.34 eV. In contrast, Ru sites display the minimal Gibbs free energy of activation ($\Delta G_{H^*} = -0.07$ eV) for the adsorption and desorption processes of H* (Fig. 6a–c) [68]. This suggests a mechanism where H* intermediates are generated from Co sites and subsequently adsorbed onto the Ru sites (by migration on surface), so facilitating a variety of interactions related to electrocatalytic reaction species. This mechanism presents a broad strategy to address challenges posed by the association of different atoms sizes and scales among various species. Hence, the deliberate engineering of electrocatalytic active sites above HEA surfaces based on their multifunctionality emerges as a viable strategy to strengthen HER activities significantly. Such endeavours hold promise for the improvement of HEA catalysts.

3.1.4. *Non-precious metal based HEAs for the HER*

The exploration of economical alternatives to precious metal elements (as are normally used in electrocatalysts) has spurred research into examining multi-component alloy materials integrating cheaper, non-precious transition metals as promising electrocatalytic candidates. Nonetheless, the application of electrocatalysts based on different transition metals when used under alkaline and acidic conditions faces constraints due to their low resistance to corrosion. This challenge stems from the accumulation and consumption of electrons based on transition metals and their related compounds, owing to the presence of partially filled *d* orbitals. The distinctive attributes of HEAs, however, present significant promise for facilitating the HER process for applications spanning a broad pH range. Efficient regulation of the interactions across electrocatalyst active sites in materials is essential for improving their electrocatalytic activities. Unfortunately, our understanding of the surface chemistry around the relevant reaction species and catalytic sites on HEAs is still restricted. This has limited the development of HEAs in a wider sense. Zhu et al. suggested a novel approach in thinking dominated by electronegativity considerations to make structural adjustments to the HEAs (Fig. 7a) [69]. This innovative strategy utilized Mn, Co, Cu, Ni, and Fe as the fundamental raw materials to fabricate a simple FCC-based HEA via the polymeric nanoreactor. Through this method, the internal charge density was found to be higher at Cu and Ni active

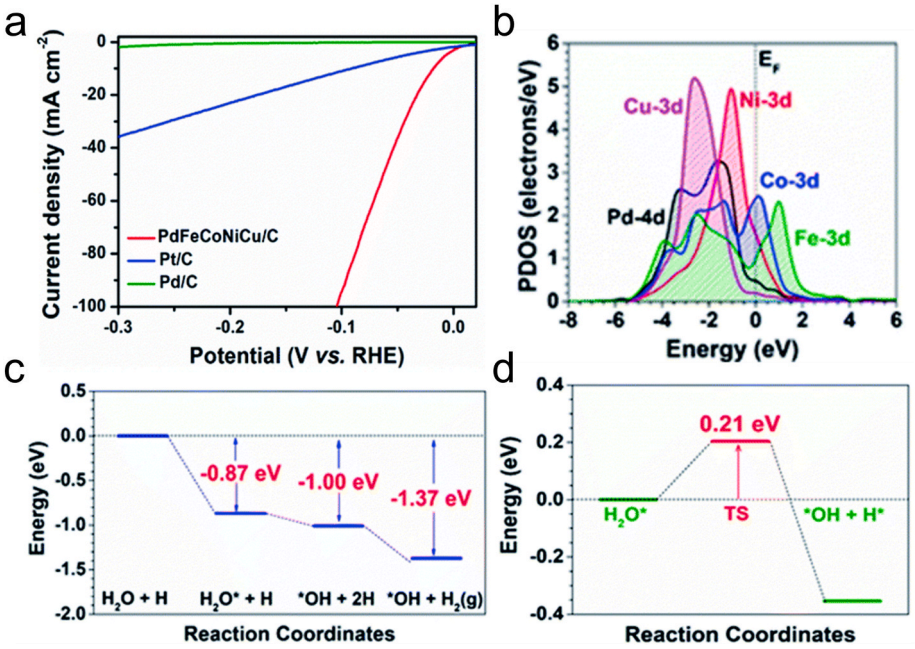

Fig. 5. (a) HER polarization curves of PdFeCoNiCu/C, Pt/C, and Pd/C in 1.0 M KOH solution (Potassium hydroxide (KOH, 90 %) was purchased from Aladdin). (b) The PDOSs of the HEA surface. (c) The energetic route of the HER process in alkaline environments. (d) The activation barriers of water splitting during the HEA process. Reprinted with permission from Ref. [67]. Copyright 2021 Royal Society of Chemistry.

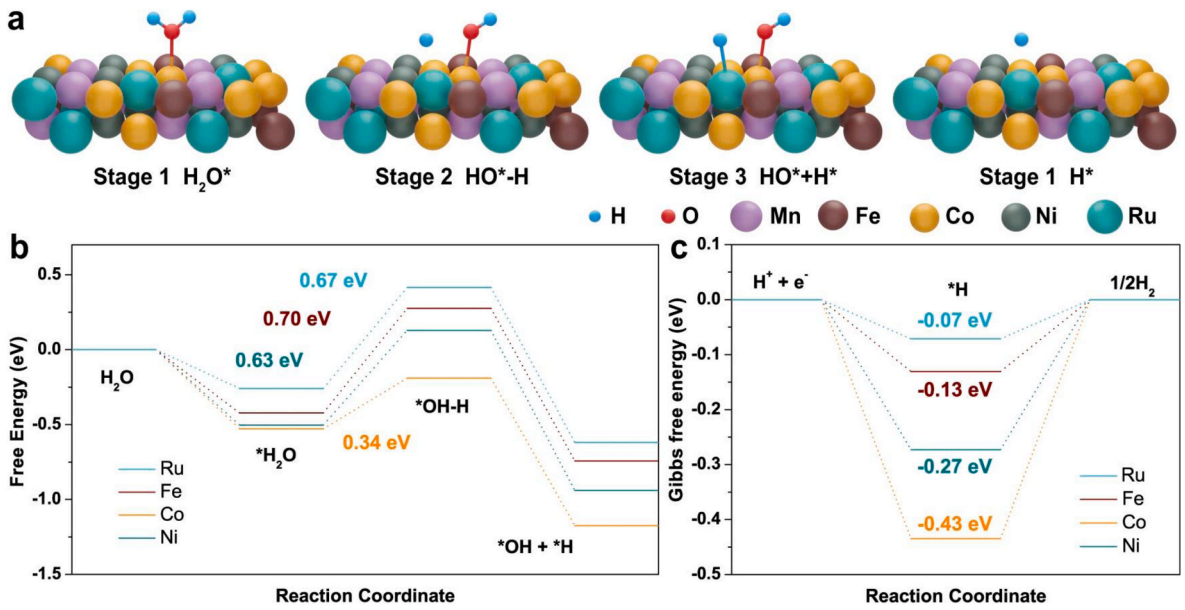

Fig. 6. (a) The atomic configurations on catalytic sites of FeCoNiMnRu HEA at the four stages during H_2O dissociation. (b) Reaction energy profile for water dissociation on various catalytic sites of the FeCoNiMnRu HEA surface. (c) Gibbs free energy (ΔG_{H^*}) profiles on various catalytic sites of the FeCoNiMnRu HEA surface. Reprinted with permission from Ref. [68]. Copyright 2022 Nature Publishing Group.

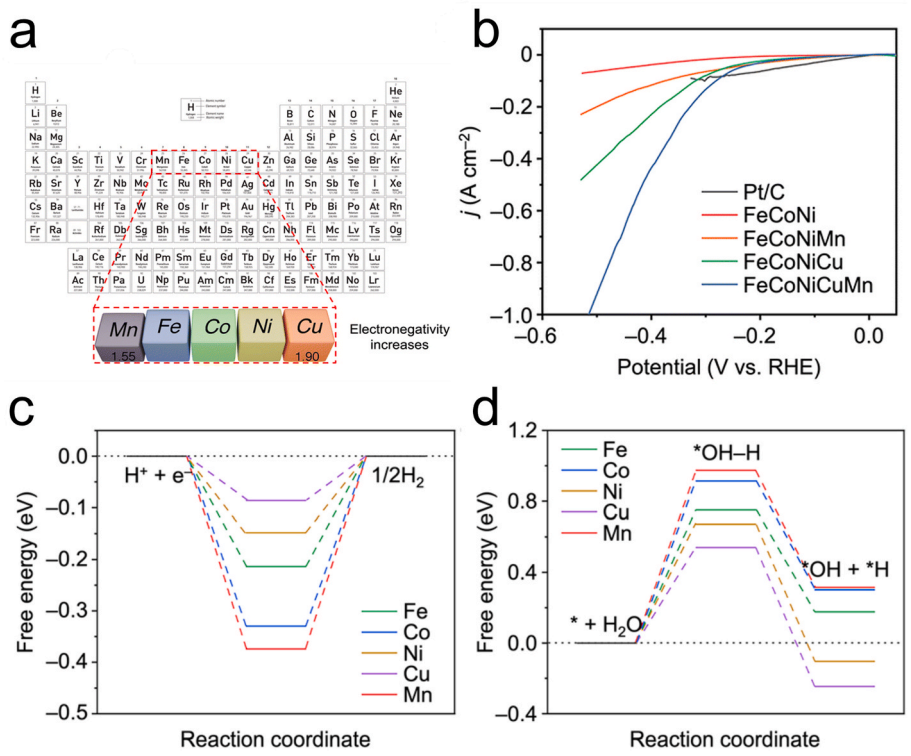

Fig. 7. (a) The electronegativity order of Mn, Fe, Co, Ni, and Cu metals. (b) Polarization curves of the FeCoNi, FeCoNiMn, FeCoNiCu, and FeCoNiCuMn HEA catalysts in a 1.0 M KOH aqueous electrolyte (KOH was purchased from Sigma-Aldrich) for the HER process. (c) The calculated energy barriers of water dissociation (ΔG_{*H2O} - ΔG_{*OH}) and (d) Gibbs free energy (ΔG_{H^*}) profiles in the HER process on Fe, Co, Ni, Cu, and Mn active sites. Reprinted with permission from Ref. [69]. Copyright 2023 Royal Society of Chemistry.

sites, while being lower at Co, Fe, and Mn catalytic sites. Moreover, inactive Cu sites were converted into active sites with enriched charge in the HER process, which led to decreased adsorption energies for all electrocatalytic species, original reactants, and final products. Leveraging the competitive priority adsorption, these HEAs displayed exceptional catalytic activities during the HER process (Fig. 7b), along with notable cycling durability. Density functional theory (DFT) simulations related to various electrocatalytic active sites based on the FeCoNiCuMn HEA further confirmed that Cu sites emerge as catalytic active sites with abundant electrons in the HER process (Fig. 7c–d).

Electrode materials employed with microstructures have an interaction with insulating polymers to preserve electric connectivity, which

frequently yields suboptimal electrocatalytic activities in terms of constraints in charge transfer and mass transport capabilities. In response to these challenges, a modifiable and simple alloying & dealloying approach for HEA materials presents a broad pathway into the large-scale manufacturing of self-supported electrodes based on these nanoporous HEAs. For example, a multi-component CuAlNiMoFe HEA material with a microporous surface integrated onto a Cu framework, has been devised as a superior catalyst in the alkaline and neutral HER process (Fig. 8a–b) [70]. This experiment was conducted through arc-melting pristine elemental Cu and Al combined with equimolar quantities of Fe, Ni and Mo metals. A sequential engineering dealloying process in KOH electrolyte yielded a stratified microstructural nanoporous Cu framework via a two-stage etching method. The sequential dealloying method involved dissolving the α-Al phase from the Al_5Mo, $Al_{13}Fe_4$, and Al_3Ni deposits, along with the etching of Al_2Cu. Consequently, an in situ outer layer HEA composed of CuNiMoFe was simultaneously synthesised on the surface. The resulting CuAlNiMoFe electrode demonstrated exceptional electrocatalytic efficiency in the acidic-free HER process which was attributed to the reconstructed HEA nano-surface. The integration of diverse metals such as nickel, molybdenum, iron, and copper into HEAs facilitated the creation of multi-functional catalytic active sites to allow water dissociation and for the adsorption & desorption of activated hydrogen reaction species (Fig. 8c–d). Moreover, the stratified microporous Cu framework served as a support, facilitating swift charge transfer and effective delivery of various atoms and ions. The manufactured CuAlNiMoFe electrode exhibited notable electrocatalytic ability, achieving (at different pHs) very low overpotentials of roughly 183 and 240 mV at current densities of around 100 and 1840 mA cm^{-2} in a buffer solution at pH = 7 and 1.0 M KOH, respectively for the HER process. These results surpassed the electrocatalytic activities of numerous, reportedly cutting-edge non-noble catalytic materials. Utilizing their fabrication of the CuAlNiMoFe HEA material as a foundation, this research team proceeded to expand their methodology to produce a self-supported integral nanoporous NiFeCoCuTi HEA, which was embedded into a multi-porous Ni framework via an alloying and dealloying technique (Fig. 9a–b) [71]. This innovative electrode design capitalizes on the existence of numerous electrocatalytic active sites which are designed to improve water dissociation and accelerate the interaction of H* catalytic intermediates to ultimately produce H_2. Consequently, the NiFeCoCuTi HEA electrode exhibited remarkable electrocatalytic efficacy in the HER process under alkaline conditions. It demonstrated a minimal overpotential value of only 209 mV and attained a substantial current density of 2 A cm^{-2} (Fig. 9c), while retaining remarkable durability over a prolonged usage time of 240 h in a solution of 1.0 M KOH (Fig. 9d). These studies underscore the promising prospects of the HEA electrode based on NiFeCoCuTi which emerges as a very productive and long-lasting electrocatalyst when used in alkaline-based HER reactions.

3.2. High-entropy alloys (HEAs) for the oxygen evolution reaction (OER)

3.2.1. Introduction to the OER

The electrocatalytic reaction of water splitting has the OER process as one of the half-cell reactions. This proton-electron conversion process involves the generation and desorption of various oxygen-related reaction species, as illustrated in Fig. 10a [72–74]. The relevant reaction equations are listed below:

Overall reaction:

$$2H_2O \rightarrow 2H_2 + O_2 \quad (1b)$$

Anode reaction under acidic situations:

$$2H_2O_{(l)} \rightarrow 4H^+ + O_{2(g)} + 4e^- \quad (9)$$

OER mechanism under acidic situations:

$$M + H_2O_{(l)} \rightarrow MOH + H^+ + e^- \quad (10)$$

$$MOH \rightarrow MO + H^+ + e^- \quad (11)$$

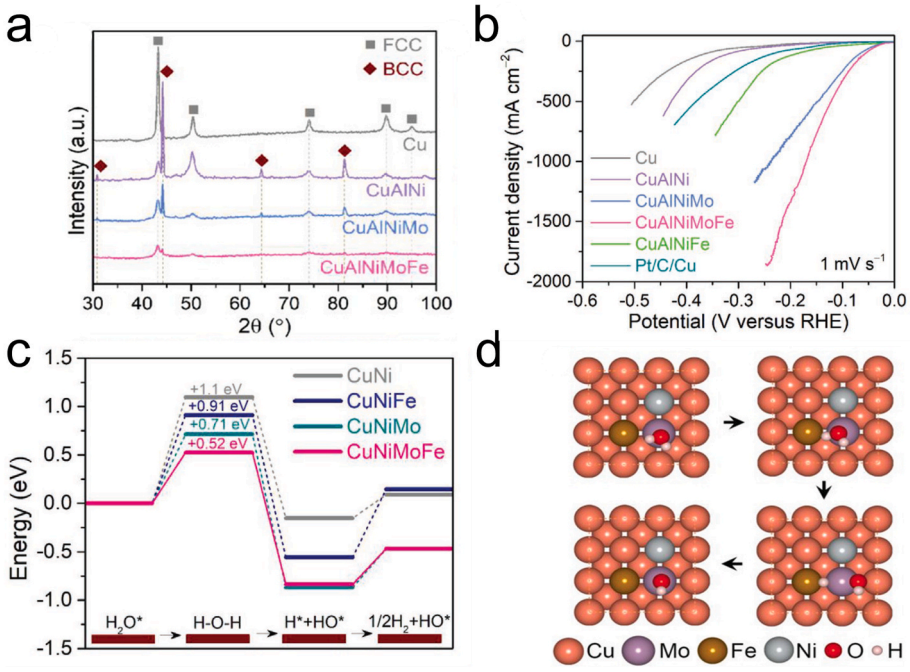

Fig. 8. (a) X-ray diffraction (XRD) patterns of as-dealloyed nanoporous Cu, CuAlNi, CuAlNiMo, and CuAlNiMoFe electrodes, where there appear newly formed diffraction peaks of BCC phase in the three multielemental alloys and their intensity decreases with the addition of Mo and Fe atoms. (b) Polarization curves for nanoporous Cu, CuAlNi, CuAlNiMo, CuAlNiMoFe, CuAlNiFe electrodes, comparing with that of nanoporous Cu supported Pt/C (Pt/C/Cu) in 1.0 M KOH electrolyte. Scan rate: 1 mV s^{-1}. (c) Reaction energy chart of water dissociation on surface CuNi, CuNiFe, CuNiMo, and CuNiMoFe alloys at different stages of the reaction, wherein the high-entropy CuNiMoFe alloy shows the lowest energy barrier for water dissociation. (d) Surface configuration of high-entropy CuNiMoFe alloy at the four different stages during the dissociating process of H_2O to H* and HO*. Reprinted with permission from Ref. [70]. Copyright 2020 Wiley.

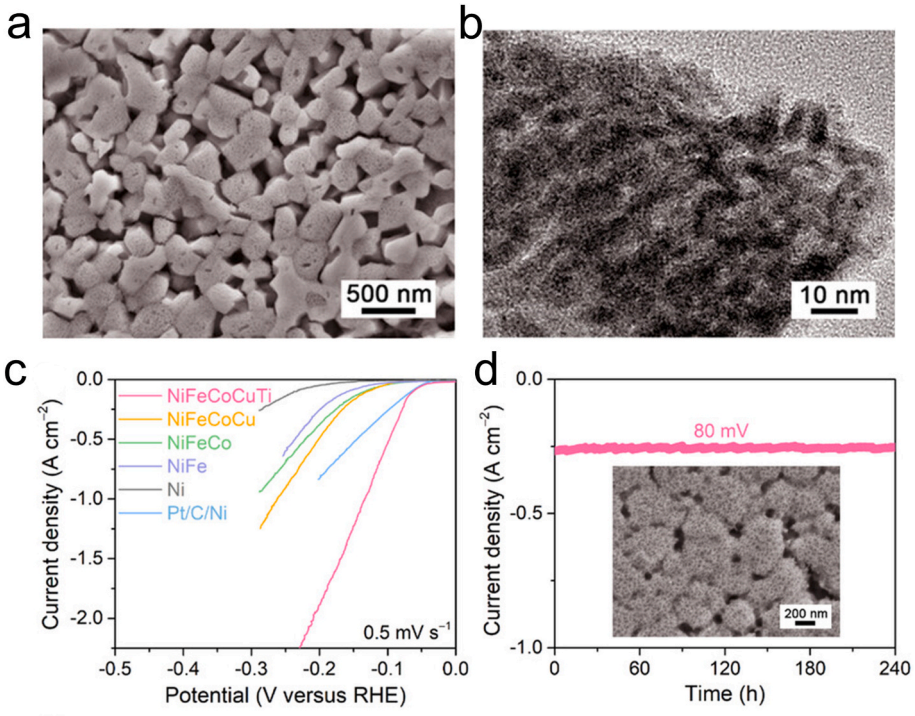

Fig. 9. Representative SEM image (a) and TEM image (b) of column-structured nanoporous high-entropy NiFeCoCuTi electrode. (c) Typical HER polarization curves for nanoporous NiFeCoCuTi, NiFeCoCu, NiFeCo, NiFe, and bare Ni electrodes, as well as commercial Pt/C nanocatalysts immobilized on nanoporous Ni (Pt/C/Ni). Electrolyte: 1.0 M KOH solution. Scan rate: 0.5 mV s^{-1}. (d) Long-term stability of nanoporous high-entropy NiFeCoCuTi electrode at overpotential of 80 mV for 240 h in 1.0 M KOH electrolyte. Reprinted with permission from Ref. [71]. Copyright 2023 Wiley.

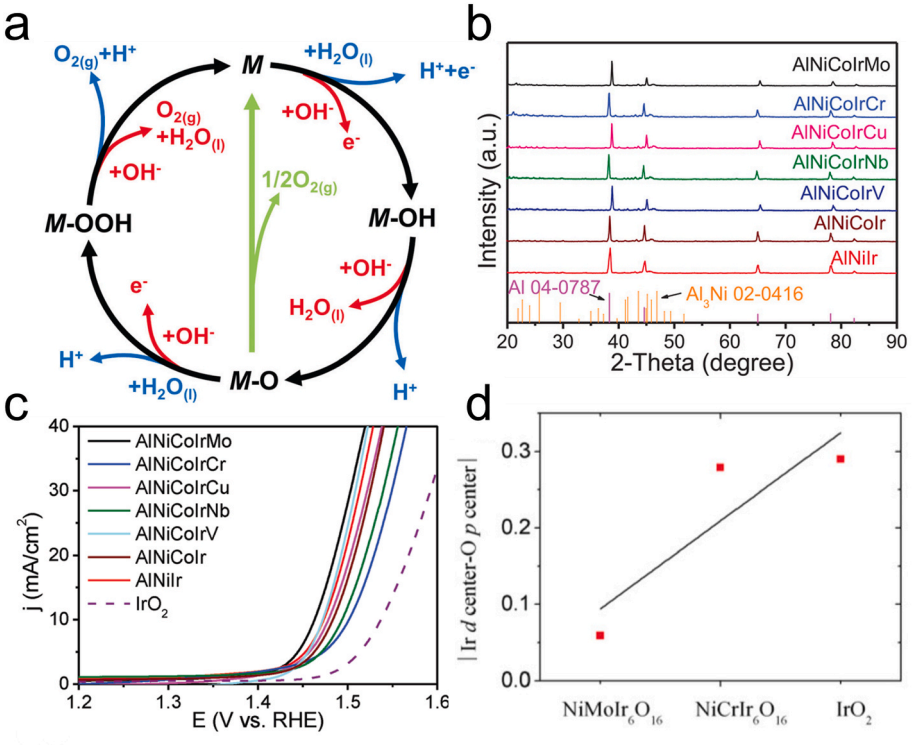

Fig. 10. (a) OER mechanism under acid (blue route) and alkaline (red route) situations. Reprinted with permission from Ref. [80]. Copyright 2017 Royal Society of Chemistry. (b) XRD patterns of the different alloys. The standard positions of Al and Al_3Ni are included for comparison. (c) OER polarization curves of all fabricated alloys and IrO_2. (d) The distinction of the *d*-band centre of metal Ir and the *p*-band centre of element O for every condition, demonstrating the strength of the covalency of the metal-oxygen bond. Reprinted with permission from Ref. [98]. Copyright 2019 Wiley. (For interpretation of the references to colour in this figure legend, the reader is referred to the Web version of this article.)

$$2MO \rightarrow 2M + O_{2(g)} \quad (12)$$

$$MO + H_2O_{(l)} \rightarrow MOOH + H^+ + e^- \quad (13)$$

$$MOOH \rightarrow M + O_{2(g)} + H^+ + e^- \quad (14)$$

Anode reaction under alkaline situations:

$$4OH^- \rightarrow O_2 + 2H_2O_{(l)} + 4e^- \quad (15)$$

OER mechanism under alkaline situations:

$$M + OH^- \rightarrow MOH + e^- \quad (16)$$

$$MOH + OH^- \rightarrow MO + H_2O_{(l)} + e^- \quad (17)$$

$$2MO \rightarrow 2M + O_{2(g)} \quad (18)$$

$$MO + OH^- \rightarrow MOOH + e^- \quad (19)$$

$$MOOH + OH^- \rightarrow M + O_{2(g)} + H_2O_{(l)} + e^- \quad (20)$$

A significant obstacle during this reaction is the substantial overpotential required for the OER, which acts as a bottleneck and hampers the efficiency of water decomposition. The development of strongly effective catalysts necessitates a comprehensive understanding of the OER mechanism. Traditionally, there were two different mechanisms have been taken into account: the lattice oxygen-mediated mechanism (LOM) and the adsorbate evolution mechanism (AEM) [75–77]. The inherent bond interactions (M−O) among species (M-OOH, M−OH, and M−O) are pivotal in identifying the whole of the electrocatalytic performance related to the OER process [78–80]. In alkaline-media-based electrolysis, the hydroxyl group undergoes oxidation, leading to the conversion of the hydroxyl group into O_2 and H_2O. In contrast, the OER process under acidic conditions involves the challenging task of breaking the robust covalent O–H bond in H_2O, leading to the consequently sluggish reaction kinetics [81,82]. Alkaline OER electrocatalysts commonly employ oxides and hydroxides based on transition metals, whereas acidic OER electrocatalysts typically rely on alloys which contain two or three elements, primarily composed of non-precious metals along with other costly metals such as Ru and Ir [83,84]. Nevertheless, employing multi-compositional alloys has shown promise in improving the durability and efficiency of the OER electrocatalysts. Particularly, HEAs with nanostructures stand out as favourable candidates, benefiting from the abundant electrocatalytic active sites and substantial reaction surface areas. The different composition enables for fine-tuning of the electronic features above the surface of HEAs, ultimately affecting electrocatalytic performance [85].

3.2.2. Design strategy for better OER electrocatalysts

The OER process in electrochemical science is complex encompassing various reaction intermediates. When catalysed via conventional catalytic materials available, the performance of these materials can be constrained due to the size of various reaction species [86–88]. Hence, for the effective improvement of the OER processes, it is essential to judiciously tune the composition and proportion of the HEA electrocatalysts to regulate the concentration of catalytic active sites. Attaining superior OER performance necessitates the application of multifunctional electrocatalytic active sites capable of interacting with a variety of reaction intermediates. Through optimizing the adsorption distributions of HOO* and HO*, a strengthening of OER activities can be realised [89,90]. The synergies realisable with HEAs are able to modify charge distribution environment and hence influence bonding, which results in an ideal binding energy for reaction active species which positively influences OER performance [91–94]. Although Ru, Ir, and their oxide catalysts exhibit outstanding electrocatalytic abilities in the OER process, their application is constrained due to their high expense. Notably, metal oxides or hydroxides, instead of other unstable reaction intermediates, contribute to the exceptional observed OER electrocatalytic activities [85,95]. Given that alloyed electrocatalysts generate reaction active species via surface reconstruction, overall binding energies of oxygen-related catalytic intermediates can be decreased, so it becomes significant to the exploitation of durable and effective electrocatalysts used on the OER process [96,97]. Thus, when considering the design of HEAs for OER processes, there could be a potential option for some specific elements to undermine the size of different reaction species.

3.2.3. Precious-metal based HEAs for the OER

Several research works have shown that OER electrocatalytic performance containing Ir-related alloys give very good results. However, due to the expense and other limitations associated with Ir, there is a growing interest in expanding the suite of multi-metallic electrocatalysts which have a decreasing amount of Ir in them with the aim of maintaining the electrocatalytic activity or even improving it in order to achieve cost advantages. In a study by Jin et al., a controlled doping technique was utilized to fabricate a range of high-entropy alloys with multi-porous microstructures, specifically focusing on quinary AlNiCoIrX compositions, where X represents various elements such as Cr, Nb, V, Mo, and Cu (Fig. 10b) [98]. Of specific note was the multi-porous AlNiCoIrMo HEA, which indicated excellent catalytic performance in the OER experiments. It showed an overpotential of about 233 mV at a current density of 10 mA cm^{-2}, surpassing other HEAs such as AlNiCoIrCr, AlNiCoIrNb, AlNiCoIrCu, and AlNiCoIrV (Fig. 10c). The enhanced OER performance were ascribed to the doping of V and Mo in the HEAs which improved activity. In contrast, the inclusion of Cr and Nb had a detrimental effect on electrocatalytic activity. Computational studies through DFT also confirmed these experimental results (Fig. 10d), which indicates that doping with metals X (especially Mo) strengthened the covalent Ir–O bond present, leading to remarkable oxygen evolution abilities.

When comparing with alkaline conditions, acidic environments without hydroxyl ions were shown to contribute to a heightened energy demand for disrupting the robust covalent bonds within H_2O that leads to the release of OH^- [99]. Consequently, a substantial energy input is required to activate the OER process in acidic solutions. However, studies have demonstrated that catalysts based on Ru display outstanding activities, promoting the OER process even within acidic environments. In line with this, Zhu et al. conducted a series of experiments revealing that modifying the temperatures of crystallization and varying metal components can enhance OER effectiveness. Under their investigation, they fabricated microstructural FeCoNiIrRu high-entropy alloy nanoparticles on the surface of electro-spun carbon nanofibres (CNFs) through an *in situ* synthesis (Fig. 11a) [100]. By employing in situ analysis approaches, they also suggested a robust thermodynamic force of these electrocatalysts which could accelerate phase transitions, thereby improving OER performance. This study achieved an extremely low overpotential of 241 mV at a current density of 10 mA cm^{-2} in a 0.5 M H_2SO_4 solution (Fig. 11b). Furthermore, the sluggish diffusion effect of HEAs contributed to superior durability through the considerable restriction of metals dissolution and leaching (Fig. 11c). DFT simulation illustrated the increase of charge density from lower electronegativity elements (Ni, Fe, and Co) to higher electronegativity elements (Ru and Ir) in the FeCoNiIrRu nanoparticles. This phenomenon accelerated the conversion from intermediate *OOH to oxygen along with improving Ru and Ir performance during the OER process (Fig. 11d).

More importantly, electrocatalysts (especially HEAs) can employ several self-reconstruction techniques in durability experiments such as in situ oxidation, surface dissolution, dissolution & redeposition, and a mix of these above processes. The challenging issue is how HEAs retain their remarkable effectiveness, although there is a formation of the oxide layer (by the self-reconstruction approach) on HEAs surfaces. In an investigation by Huang et al., a series of experiments of the FeCoNiRu HEA with a long-lasting OER durability test at 10 mA cm^{-2} for 40 h were

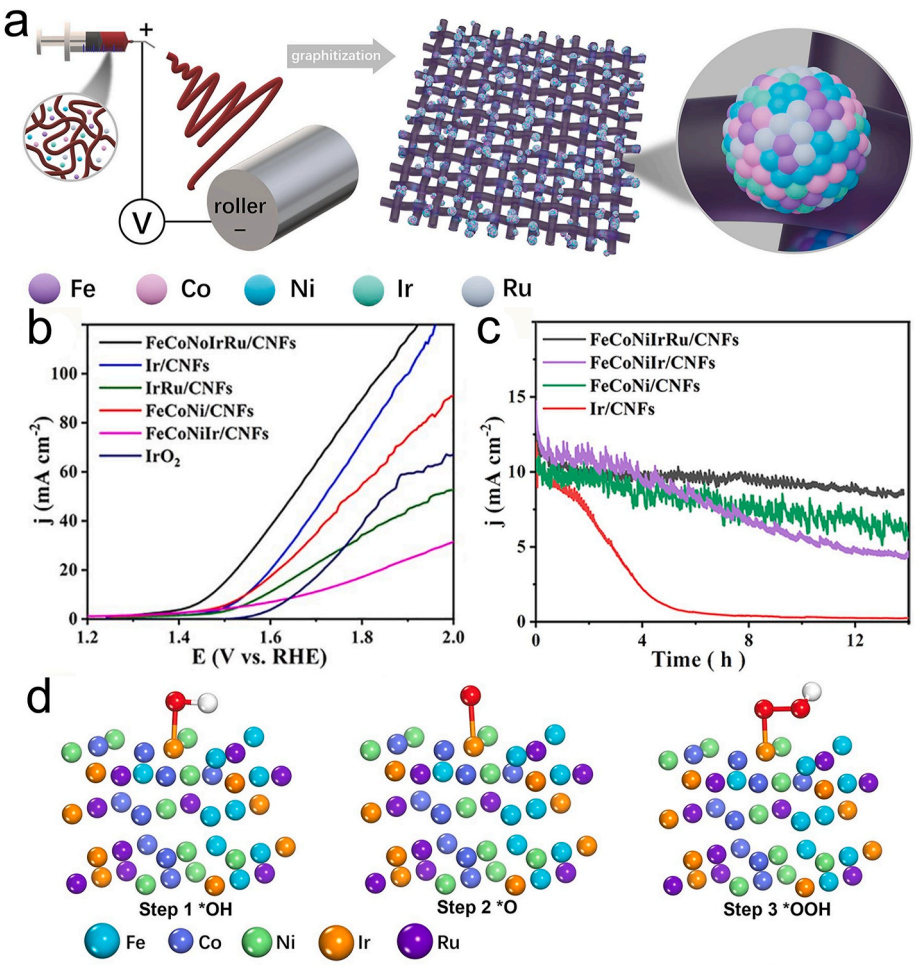

Fig. 11. (a) Typical synthesis procedure for the FeCoNiIrRu/CNFs by combining the electrospinning and graphitization process. (b) OER polarization curves at geometric current density of 20 mA cm^{-2} of prepared electrocatalysts obtained in 0.5 M H_2SO_4 solution. (c) Chronoamperometry (i–t) curves of FeCoNiIrRu/CNFs, FeCoNiIr/CNFs, FeCoNi/CNFs and Ir/CNFs obtained at current density of 10 mA cm^{-2}. (d) The adsorption states of *OH, *O, and *OOH of the OER process on Ir site of FeCoNiIrRu HEA nanoparticles. Reprinted with permission from Ref. [100]. Copyright 2021 Elsevier.

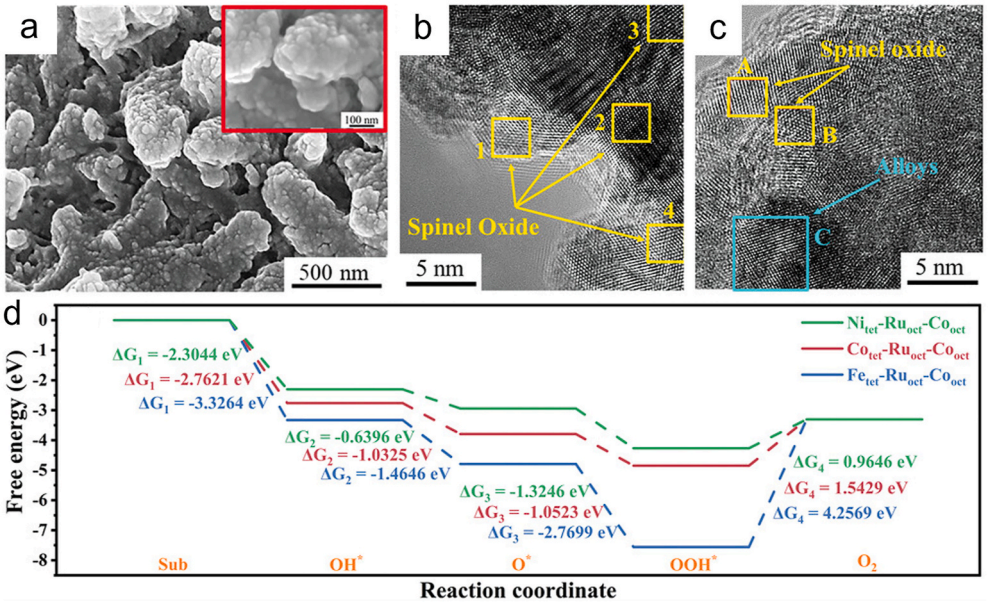

Fig. 12. Field-emission SEM (FESEM) (a), and high-resolution TEM (HRTEM) images (b) and (c) of FeCoNiRu electrocatalysts after the OER durability experiments. (d) OER energy illustration of hollow sites with various tetrahedron metal elements. Reprinted with permission from Ref. [101]. Copyright 2023 Wiley.

explored [101]. After these long-lasting tests, surface analysis of the HEAs using SEM and TEM unveiled the formation of a thin oxide layer that seems to be covering the whole FeCoNiRu HEA surface (Fig. 12a–c). High-resolution TEM (HRTEM) was used to show that the oxide layers were spinel oxide nanostructures of (Ni, Fe)(Co, Fe, Ru)$_2$O$_4$. DFT calculations clarified that the outstanding OER activities of these spinel oxide nanostructures resulted from inherent hollow electrocatalytic active sites that were distributed over the surface of the catalysts (Fig. 12d). Moreover, these hollow electrocatalytic active sites still persisted in the spinel oxide microstructures when exposed to outside current. Thus, these catalytic reaction sites retained receptiveness to hydroxide ions and benefited the OER process in the durability experiments.

3.2.4. *Non-precious metal based HEAs for the OER*

The effectiveness of electrocatalysts in the OER process is affected by a number of factors, such as elemental composition, morphology, oxides/hydroxides nanostructures, surface atom binding energy, and *d*-orbital electron numbers in the transition metal elements used [102, 103]. To explore the range of economical and durable electrocatalysts available it is necessary to consider a large range of transition metal elements in order to make HEAs that hold promise. In a study by Qiu et al., a simple technique was employed to generate a series of homogeneous nanoporous HEAs (np-HEAs), with a particular focus on AlNiCoFeX compositions (X = Cr, Mo, Nb) (Fig. 13a). These np-AlNiCoFeX HEAs were found to exhibit superior OER performance (with lower overpotentials) when used in 1.0 M KOH, surpassing those of ternary or even quaternary alloys that had been used previously (Fig. 13b) [104]. The enhanced OER performance observed in the AlNiCoFeX HEAs was attributed to more an electronic influence rather than the high-entropy effect. The electronic influence was suggested by spin-dependent Partial Density of States (PDOSs) calculations carried out in accordance with the e_g-orbital filling rule (which describes the order in which electrons populate atomic orbitals) as used for rationalising why oxygen evolution processes occur (Fig. 13c). This implies that the multi-compositional transition metal oxides provide more scope for catalytic surface reaction variety, which surpasses the restrictions associated with common binary and ternary alloys. This factor therefore boosts electrocatalytic performance in the OER processes [105]. Aside from the influence of electronic structure, lattice distortion was also identified as a considerable factor in enhancing the electrocatalytic activity of OER on the HEAs. Huang et al. confirmed this effect through the research of MnFeCoNiCu HEA nanoparticles [106]. A large degree of lattice distortion was caused via lattice mismatch which benefitted OER activities (Fig. 14a–f). This underscores the significance of surface reconstruction for HEA-based electrocatalysts and so provides valuable insights for advancing the field.

Cui and colleagues conducted a series of experiments on the OER process of two different HEAs, FeCoNiCrAl and FeNiMnCrCu. The aim of the research was to assess how the constituents of these alloys affect OER performance [107]. The research revealed that Cu, with a fully-filled *d* orbital, acts to accelerate charge transfer to that of other component elements, ultimately reducing the number of defects and whole bonding energy. Meanwhile, Mn exhibited a favourable affinity to O atoms due to its large atomic radius, promoting charge transport and enhancing the OER performances by matching defect numbers. The FeNiMnCrCu HEA displayed a notable abundance of surface active sites, which promoted efficient reactant adsorption and exhibited a substantial residual strain so contributing to enhanced OER performance at lower overpotential values (Fig. 14g). Experimental outcomes also validated the theoretical calculation, which further confirmed the superior OER performance of FeNiMnCrCu alloy (Fig. 14h). Specifically, these results showed the improved adsorption of catalytic intermediates and strengthened charge transfer effectiveness on the HEA surface.

In relation to HEAs, the scientific understanding of the surface reconstruction methodology in the OER process remains an understudied topic compared to that of the more broadly investigated materials [108]. In research by Chen et al., the influence of an electrocatalytic cycling approach based on surface reconstruction was demonstrated [109]. In this work, the CrMnFeCoNi HEA films were deposited onto both Ni foam (NF) and carbon cloth (CC) through pulsed laser deposition techniques (Fig. 15a). The findings revealed that the cyclic voltammetry

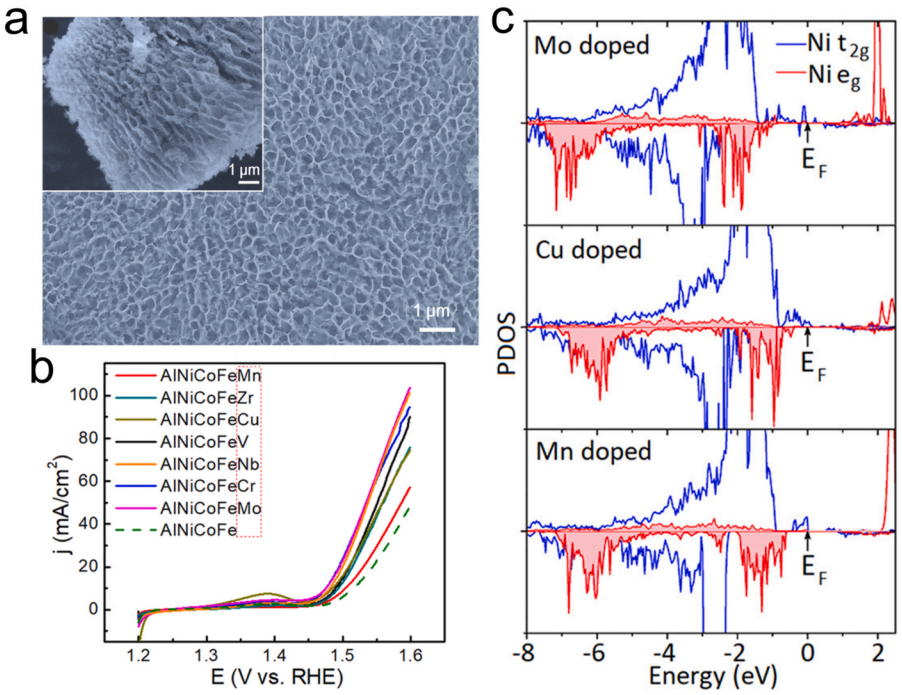

Fig. 13. (a) Plane-view and section-view SEM image (inset in panel a) of the nanoporous AlNiCoFeMo. (b) LSV curves showing the oxygen evolutions of different nanoparticle HEA electrodes. The PDOSs onto the *d* states of single Ni element on the octahedral site close to the dopant (c) for Mn, Cu, and Mo, respectively, from bottom to top. Reprinted with permission from Ref. [104]. Copyright 2019 American Chemical Society.

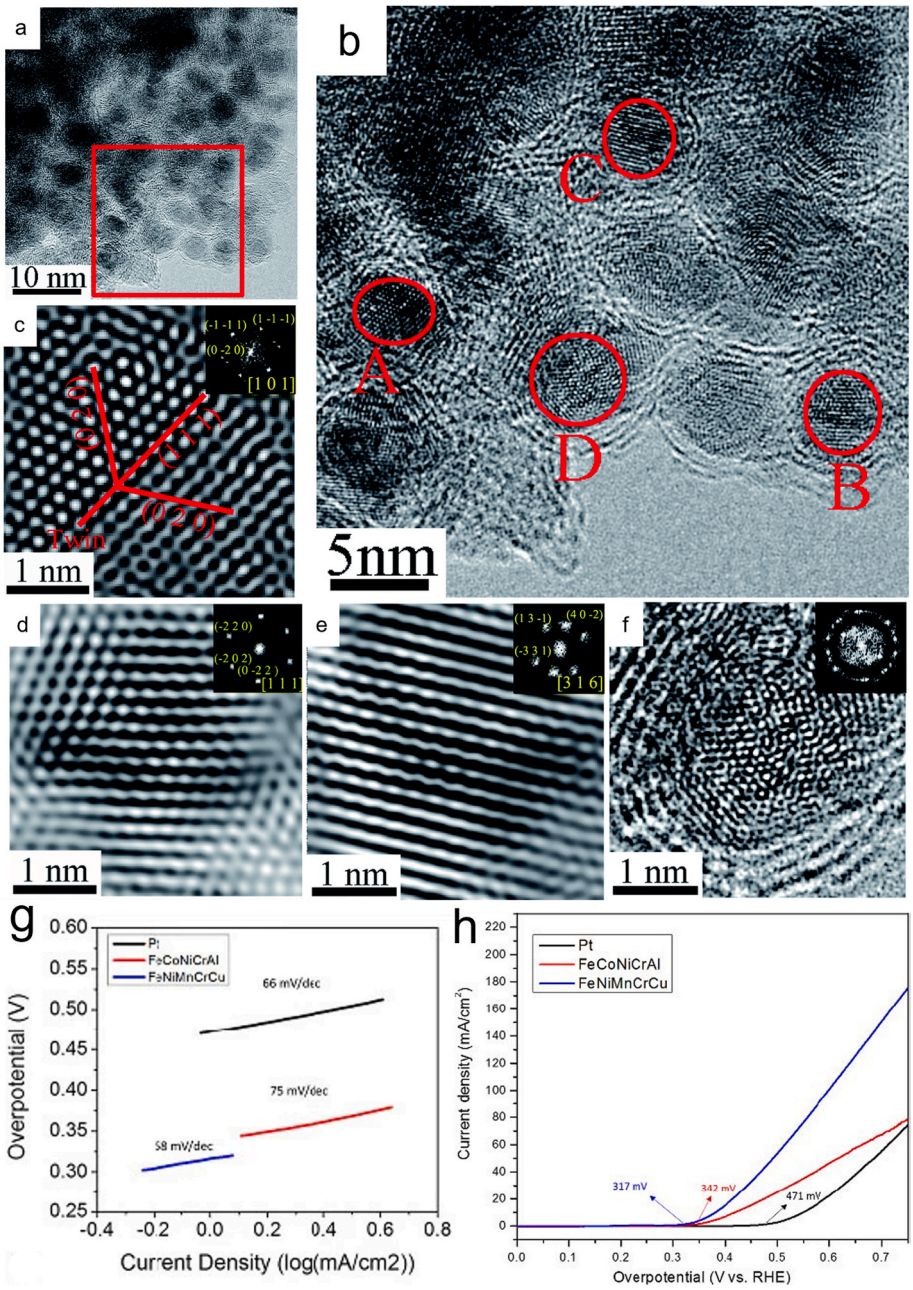

Fig. 14. (a) A bright-field TEM image showing the dispersion of HEA nanoparticles at a low magnification. (b) Zoom-in TEM image taken from the squared area marked in (a). High-resolution TEM images showing the atomic lattice of particle A (inset: FFT pattern) (c), particle B (inset: FFT pattern) (d), particle C (inset: FFT pattern) (e), and particle D (inset: FFT pattern) (f). Reprinted with permission from Ref. [106]. Copyright 2020 Royal Society of Chemistry. The Tafel slopes (g) and the OER polarization curves (h) of FeCoNiCrAl and FeNiMnCrCu electrodes, respectively. Reprinted with permission from Ref. [107]. Copyright 2018 Springer.

(CV) method (which involves potential cycling between two voltage limits) brought about the surface reconstruction of the HEA films, resulting in the generation of intense active hydroxide or oxyhydroxide reaction intermediates on the surface of the HEAs (Fig. 15b–c). The CV-activated HEA/NF and HEA/CC electrodes were found to demonstrate outstanding electrocatalytic performance in the OER progress which consequently occurred with very low overpotential values (287 mV and 315 mV at a current density of 10 mA cm^{-2}, respectively). Additionally, these HEA films (after CV-assisted surface reconstruction) exhibited notable durability when subjected to a chronoamperometric (CP) characterization, lasting for 360 h in total (300 h at a current density of 10 mA cm^{-2} and an extra 60 h at a current density of 100 mA cm^{-2}) and 300 h (at a current density of 10 mA cm^{-2}) was observed based on the HEA/NF and HEA/CC materials, respectively (Fig. 15d). Electrochemical impedance spectroscopy (EIS) outcomes suggested that HEA/CC-a1 (the 1st CV-activated HEA film) displayed a smaller interfacial resistance (R_{int}) value (0.1 Ω cm^2) than that of HEA/CC, implying faster OH^- adsorption and reaction species formation in the interfaces between electrodes and electrolyte. The heightened activities observed in this system could be ascribed to the occurrence of the reactive hydroxide or oxyhydroxide reaction intermediates which would have been generated as a result of the surface reconstruction, offering extra catalytic active sites during the OER process and facilitating relevant reaction species to form which would aid the OER process.

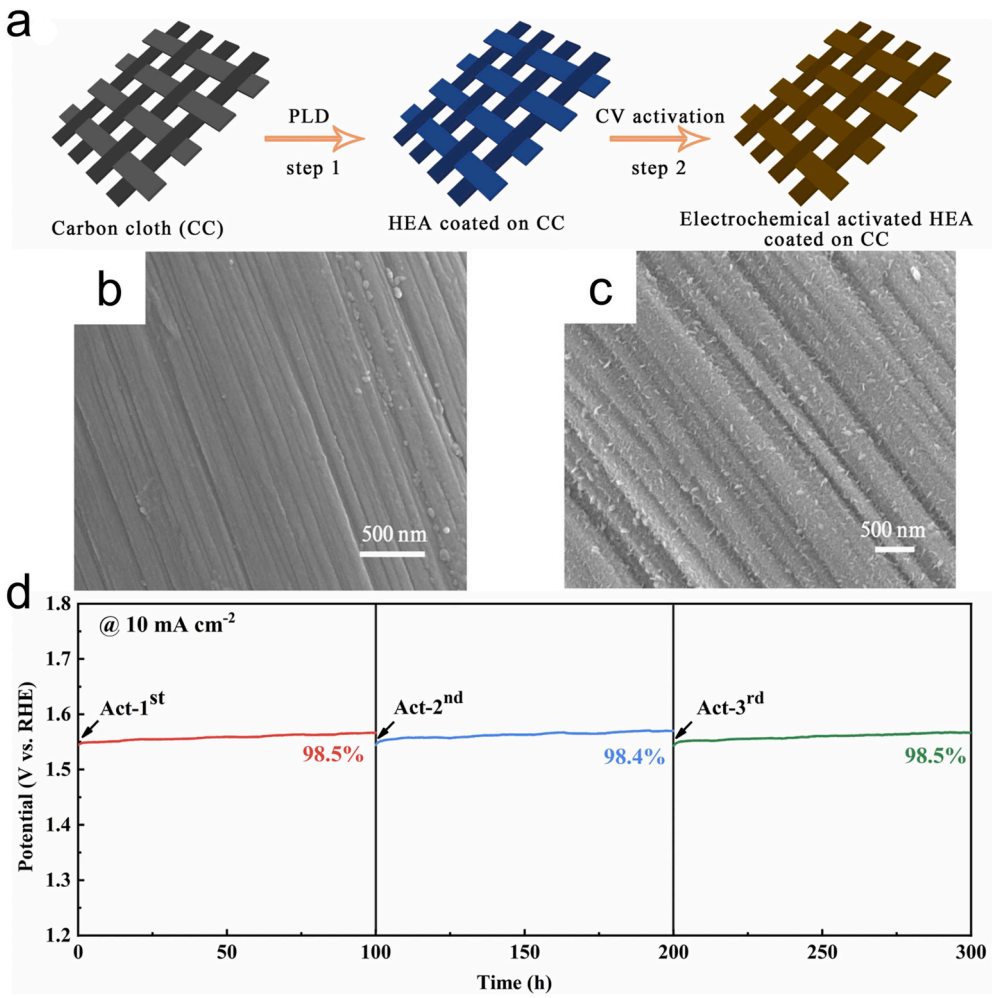

Fig. 15. (a) The schematic diagram of deposition process of HEA films on CC. (b) SEM image of HEA/CC. (c) SEM image of HEA/CC-a1. (d) Long-term CP durability test of CrMnFeCoNi HEA working electrode for OER at 10 mA cm^{-2} for 300 h with periodic activation step. Reprinted with permission from Ref. [109]. Copyright 2022 Elsevier.

4. Challenges and limitations of HEA electrocatalysts

4.1. Stability issues

As a green and renewable energy, hydrogen energy has a sustainable development future, which can reduce the carbon emission and the use of fossil fuels. Currently, there has been considerable attention on water electrolysis for the eco-friendly manufacturing of hydrogen energy. Nevertheless, water splitting is severely constrained due to the inherent energy barrier, which results in a low effectiveness of hydrogen generation. Thus, developing durable, effective, and corrosion-resistant HEA catalysts is crucial for the stable hydrogen production at high current densities and industrial-scale applications in water electrolysis [133]. Among many catalysts, HEA electrocatalysts displayed exceptional catalytic performance, which surpasses many state-out-of-art catalysts. Nevertheless, the long-term electrochemical durability for water splitting is still hard to meet the demands for industrialization [134]. The stability challenges for HEA electrocatalysts mainly include the element leaching, the structure degradation, the phase segregation, and the peeling on the surface of the electrode [135,136].

Recently, the majority of research is focused on enhancing the performance of HEA electrocatalysts while ignoring the significance of improving long-term stability. Therefore, to further explore the long-term electrochemical stability of HEAs, we suggest the following perspectives which needs attention: (i) It is significant for HEA electrocatalysts to indicate their charge and mass transfer effects, particularly for porous electrodes which can trap bubbles and cover the reaction sites. During the water splitting progress, the electrocatalytic efficiency is considerably affected through the gas evolution and the mass transfer at the interface of catalytic reactions [137]. The evolved gas sticks to the surface of electrodes, which forms bubbles that gradually cover a large part of active sites. This restricted mass transfer rate severely hinders the interactions of ions and charge at the interface, consequently lowering the catalytic kinetics. The water electrolysis rate can be improved via tuning fabrication strategies of HEA electrocatalysts, which further promotes the gas evolution on the surface of catalysts and accelerates the mass transfer at the interface. (ii) Long-term electrochemical durability mechanisms have not been well elucidated. The structure evolution and phase changes of HEA electrocatalysts are still a critical issues since these challenges restrain their commercial values in industrial applications [138]. Hence, it is necessary to explore advanced characterization techniques that can monitor local environmental changes and analyse the structure-performance relationship on the surface of HEA electrocatalysts such as phase transitions, nano-scale morphology changes, compositional element leaching, and catalyst degradation [139]. Employing *in situ* characterization techniques like *in situ* XRD, *in situ* TEM, *in situ* Raman spectra, and *in situ* infrared spectroscopy, suggests a pathway for further detection and analysis of the catalytic reaction mechanisms based on HEA electrocatalysts. These advanced techniques present a significant means to

demonstrate the complicated reactions in real time during the electrocatalytic progress, which improves our ability to establish a comprehensive understanding of HEAs' behaviour in long-term stability tests.

4.2. Scalability concerns for real-world electrolysis applications

To date, HEA electrocatalysts have indicated exceptional catalytic activities compared with that of commercial precious metal-based catalysts, which gains increasing attention for their potential to favour water electrolysis and thus deserves further exploration to meet sustainable and renewable energy requirements. Despite these great advancements, these is still a considerable gap between current research progress and demands from industrial applications [140]. The intrinsic ability to be scaled up and catalytic activities are both significant goals if industrial applications are to be realised from use of HEA electrocatalysts. There have been many publications where HEA electrocatalysts are stated as achieving superior catalytic activities (over 1 A cm^{-2}) in laboratory-scale tests. However, laboratory-scale HEA electrocatalysts are normally synthesised using limited electrode sizes (on small scale of 1 cm^2 or smaller), which makes it difficult to predict what is needed for industrial applications (where electrodes need to be on the square metre scale) [141,142], and the close control of conditions achievable at laboratory scale cannot represent the real activities that are experienced under actual commercial/industrial operations. In order to achieve transfer of HEAs electrocatalysts technology to industrial applications in environment protection and practical production, the development of fabrication approaches with high efficiency and reproducibility is also crucial. Current synthesis conditions of HEA electrocatalysts normally include high temperature, high pressure, inert gas atmosphere, and other factors which greatly restrict their industrial applications. Specifically, the casting procedure employed in the dealloying technique needs high temperatures in an inert atmosphere, which leads to more energy consumption and hence inherently higher fabrication costs. Conversely, the electrodeposition method products only a small amount of alloy powders, despite being more energetically favourable in its synthesis under room temperature conditions without an inert environment. Hence, the drive to develop highly efficient fabrication methods for HEA electrocatalysts with well-designed composition, morphology, and homogeneity has become essential for this technology to become practically useful [143].

In addition, for the industrial production of clean hydrogen, water splitting is typically conducted in water electrolysers at large current densities. However, the deployment of water electrolysers is significantly hindered due to poor activities and sluggish catalytic kinetics of the two half-reactions involved: HER and OER. Promising strategies have been proposed to solve these issues, but challenges still exist, which severely constrains industrial-scale applications based on this technology [144,145]. Firstly, although some excellent HEA electrocatalysts have already been published with fast catalytic rate and low overpotentials, most of their current densities are still lower than 300 mA cm^{-2}, which is far below the high current densities (normally over 0.5 A cm^{-2}) of satisfying industrial requirements [146]. Moreover, the severe reaction conditions of water electrolysers including the large amount of hydrogen and oxygen bubbles produced, high reaction temperatures (from 40 °C to 80 °C), and high concentrations of electrolytes, inevitably lead to the degradation of electrocatalysts and the decrease of catalytic activities in long-term industrial generation. Therefore, the better way to handle these challenges is to explore high-performance HEA electrocatalysts with industrial application potential, which further facilitates the industrialization for water electrolysis.

4.3. High synthesis costs and mass production difficulties

Numerous research has been reported on the preparation of different HEA catalysts in both precious and non-precious electrocatalytic systems. Especially, the interaction of various compositional elements in HEAs leads to the formation of active sites, which is significant in electrocatalysis [147]. The distinctive synergistic interactions between compositional elements can generate active sites, which promotes efficient bonding and anti-bonding of reaction species in water-splitting applications for both HER and OER [148,149]. In the context of precious electrocatalytic system, metals like platinum (Pt) suggests excellent catalytic performance in the HER progress due to the edge sites of the intrinsic FCC structure [150,151]. Conversely, in non-precious electrocatalytic system, the major mechanism for this system is to regulate the d-band centres to further optimize the electronic structures and catalytic activities of these HEA electrocatalysts [152].

Till now, most published HEAs include precious metals to increase the catalytic performance. Nevertheless, these employed precious metals like ruthenium (Ru), iridium (Ir), and platinum (Pt), just account around 10^{-7} % of earth's crust, which are far less abundant compared with non-precious metals. Thus, the scarcity not only leads to the corresponding high cost (e.g. Pd $38,400,000/T and Pt $28,800,000/T), but it also raises concerns regarding the sustainability of the supply for wide-scale applications. Moreover, the mining and refining progress of precious metals has detrimental effect on environment. These mentioned factors greatly constrain the industrial-scale applications of precious metals, whereas non-precious metals (such as Co (2.5×10^{-3} %), Ni (8.4×10^{-3} %), and etc.) are relatively more abundant and cost-effective (e.g. Co $33,420/T and Fe $120/T), which makes them more attractive for commercial uses. Additionally, some precious metals are more sensitive to be corroded, which further decreases their potential as stable components of HEAs in the long-term electrolysis [153]. Precious metal-free HEAs can be regarded as promising materials to ultimately substitute precious metals used in electrocatalysis. Hence, introducing non-precious metals into HEA electrocatalysts has drawn a considerable attention in the hydrogen production area.

5. Summary and outlook

In this review, we provide a concise overview of the fundamental characteristics and recent advancements in research on catalysts composed of high-entropy alloys. We delved into the electrocatalytic water splitting applications of HEAs, which focuses on the HER and OER. The remarkable electrocatalytic performances exhibited by HEAs can be ascribed to the synergistic influences arising out of the combination of multiple transition metals into an alloy which results in the creation of diverse and well-optimised active sites that act to enhance efficient electrocatalytic reactions. Despite their promising potential, the widespread utilization of HEAs into electrocatalysis face challenges stemming from the complex nature of their multi-element composition and the interactions that occur on their surfaces as a result. Therefore, further advancements in the applications of high-entropy alloys for electrocatalysis require careful consideration of these aspects. In light of this, we propose several achievable recommendations for future research in this field which are aimed at overcoming the challenges and maximising the promising applications HEAs have towards being efficacious electrocatalysts for the OER and HER.

(i) While notable advancements have been achieved in crafting HEA nanocatalysts, there exists a deficit of knowledge with respect to the precise control of constituent atom arrangements within the alloy. Furthermore, there is room for improvement in enhancing both the scale and yield of production of the HEAs. To address these challenges, the pursuit of carefully studied innovative synthetic approaches is crucial. These approaches will refine the nature of the electrocatalytically active sites, the porous distribution, and the morphology of the HEA nanostructures, ultimately leading to increased scalability and higher yield in manufacturing processes. Moreover, it is imperative for researchers to explore various preparation techniques, to go beyond the confines of HEA nanostructures to see if other HEA morphologies could be considered such as wires, bulk materials, powders, and films. HEA coatings as electrocatalytic materials should also be thoroughly investigated,

broadening the scope of their nature in various contexts. Each synthesis technique will have its distinct advantages and limitations. For example, the dealloying approach has overcome conventional constraints to successfully produce transition metal alloys. The primary benefit of dealloying lies in its cost-effectiveness and scalable fabrication capabilities. However, its drawback is the involvement of complicated processing steps, which can cause slower catalytic reaction kinetics [154,155]. Additionally, a technique termed the solvothermal synthesis operates directly through chemical/physical methods, resulting in minimal energy loss and more efficiency. Despite this efficiency, controlling the morphology and size of the fabricated HEAs remains a challenging task [156,157]. Yet another novel method called the carbothermal-shock enables the efficient fabrication of compositionally homogeneous transition metal HEAs. However, this method involves predominantly coating the synthesised HEAs on carbon-based supports like carbon paper and good carbon supports must be judiciously chosen for this purpose [158,159]. Furthermore, alternative conventional techniques for synthesizing alloys also hold promise in fabricating high-entropy alloys. Methods like arc melting, laser cladding, and thermal spraying offer viable options for the preparation of these materials. For solid samples, the arc melting has often been used as its excellent uniformity in ingot size and great production efficiency, while it has limited element selection and inevitably needs high temperatures and pressure during the process, which causes high energy consumption [160,161]. In contrast, the coatings can be produced using such techniques as thermal spraying or laser cladding. Laser cladding, known for its rapid heating and formation of a compact and homogeneous cladding layer, can be susceptible to cracking and lacks reproducibility in its formation [162,163]. On the other hand, the thermal spraying approach allows for good control of coating degree of thickness and is not constrained by the morphology and diversity of materials, though it tends to produce more porous coatings compared to those prepared by laser cladding [164,165]. It is significant for the fabrication of HEAs to develop the most effective and practical technique. Thus, it can be benefited via considering these diverse approaches (Fig. 16).

(ii) In addition, enhancing the efficiency of theoretical frameworks and experimental procedures stands as a potential avenue for expediting the identification of effective and enduring electrocatalysts. In essence this means that delving further into cutting-edge computer-aided theoretical computations and predictive methodologies holds considerable potential for advancing the field of HEAs in terms of fabrication and electrocatalytic applications [166]. The integration of high-throughput methodologies, DFT calculations, and internal synergies play a crucial role in fabricating more precisely defined HEAs which could be endowed with potentially exceptional electrocatalytic attributes [167]. The key to water electrolysis research is to illustrate the structure-performance relationship via tuning morphologies and electronic structures on the surface of electrocatalysts [168]. This point inspires for the unique design of electrocatalysts [169]. Theoretical calculation offers deep understanding of electronic structures, active sites, and atomic-level details of catalysis pathways, while the depth of insights is difficult to obtain only by experimental results [170]. Nevertheless, theoretical calculations still have their limitations as computational results are just abstract models based on real reactions, and oversimplify intricate reaction processes, which makes it difficult to identify the significant value of calculated findings. Currently, researchers are increasingly acknowledging the significance of employing element composition screening approaches for developing the latest electrocatalysts through well-optimised materials. Numerous scientific endeavours have been dedicated to the experimental and theoretical exploration of HEA electrocatalysts, aiding in the identification of HEAs interfaces and electrocatalytic active sites [66,68,147,171–176]. Based on their theoretical calculation, the most suitable position and ratio of each compositional atom in HEAs including the distance of every atom to the active sites and surrounding atoms, as well as the Gibbs free energy for reaction intermediates and pathways can be well evaluated. It also promoted the evaluation of electrocatalytically active sites, and a deeper understanding of mechanisms to optimize the adsorption energy of catalytic reaction species.

There is a most dire need from research reviewed to identify a cost-effective and time-efficient approach to arrive at realistically optimised combinations of component elements and proven interface nanostructure for electrocatalysts based on HEAs. Through computational investigations, the electronic status of elements, the extensive proportion of atoms, and the precise spatial arrangement of each atom within such systems can be clearly analysed [177,178]. Subsequently, by analysing all of the possible screening outcomes inputted, there exists the possibility of choosing the most viable elemental compositions for further exploration as part of a machine learning-based design strategy. A valuable understanding of the design of HEAs in electrocatalytic applications has been obtained based on these theoretical calculations [179]. Currently, the compositional elements of HEAs are normally selected through trial-and-error methods and DFT calculations based on first principles, rather than the predictive models supplied via machine learning. However, the exploration of novel HEAs that can surpass the inherent performance thresholds for water electrolysis is still slow without supporting by machine learning. Therefore, the development in this direction can underlying simplify the design of novel HEAs, especially for non-precious metal based HEAs, which further benefits the purpose of cost-effective fabrication and commercialization [180,181]. To optimize the desired aim of cost-effectiveness, greater emphasis is placed on the incorporation of the lower cost transition metal alloys in the compositions, where the fabrication of various materials with superior electrocatalytic activity can consequently be achieved via a synergistic integration of theoretical simulation and experimental validation [182].

(iii) Lastly, the majority of research in high-entropy alloy electrocatalysis predominantly revolves around the processes of HER and OER related to water splitting. Nevertheless, there is a notable scarcity of water-related studies addressing the hydrogen oxidation reaction (HOR) and the oxygen reduction reaction (ORR). Hence, there is a crucial need for exploration into the application of HEAs in catalysing the HOR and

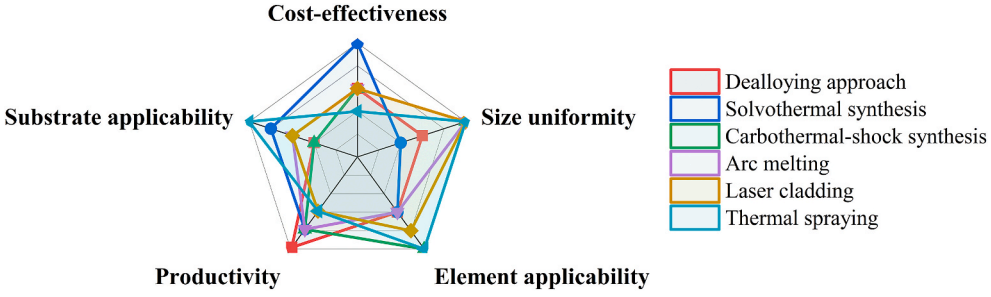

Fig. 16. Comparison of different synthetic methods for HEAs in terms of cost-effectiveness, size uniformity, element applicability, productivity, and substrate applicability.

ORR processes. Simultaneously, it is imperative to broaden the scope of HEA electrocatalyst applications beyond just water splitting reactions, which could be regarded as another research direction in the future. This expansion should also encompass various areas such as metal-air batteries and fuel cells. Essentially, this review has shown that the investigation into HEA electrocatalysts, while seemingly extensive, is still, after all considerations, in its infancy but remains a promising and fertile avenue for future research. It is anticipated that, as exploration progresses, HEAs may play a pivotal role in shaping the future landscape of electrocatalysis and so provide a partial replacement for fossil fuels which would be a major step in transforming how we achieve our energy needs.

CRediT authorship contribution statement

Z.Y. Fan: Writing – original draft, Investigation, Formal analysis. **M. Mucalo:** Writing – review & editing, Supervision, Formal analysis. **J. Kennedy:** Writing – review & editing. **F. Yang:** Writing – review & editing, Supervision, Formal analysis, Conceptualization.

Data availability

Data will be made available on request.

Declaration of competing interest

The authors declare that they have no known competing financial interests or personal relationships that could have appeared to influence the work reported in this paper.

References

[1] Tu Q, Parvatker A, Garedew M, Harris C, Eckelman M, Zimmerman JB, et al. Electrocatalysis for chemical and fuel production: investigating climate change mitigation potential and economic feasibility. Environ Sci Technol 2021;55:3240–9. https://doi.org/10.1021/acs.est.0c07309.

[2] Tang C, Zheng Y, Jaroniec M, Qiao S-Z. Electrocatalytic refinery for sustainable production of fuels and chemicals. Angew Chem Int Ed 2021;60:19572–90. https://doi.org/10.1002/anie.202101522.

[3] Centi G, Perathoner S, Genovese C, Arrigo R. Advanced (photo)electrocatalytic approaches to substitute the use of fossil fuels in chemical production. Chem Commun 2023;59:3005–23. https://doi.org/10.1039/D2CC05132J.

[4] Sultan S, Tiwari JN, Singh AN, Zhumagali S, Ha M, Myung CW, et al. Single atoms and clusters based nanomaterials for hydrogen evolution, oxygen evolution reactions, and full water splitting. Adv Energy Mater 2019;9:1900624. https://doi.org/10.1002/aenm.201900624.

[5] Boettcher SW, Surendranath Y. Heterogeneous electrocatalysis goes chemical. Nat Catal 2021;4:4–5. https://doi.org/10.1038/s41929-020-00570-1.

[6] Kibria MG, Edwards JP, Gabardo CM, Dinh C-T, Seifitokaldani A, Sinton D, et al. Electrochemical CO_2 reduction into chemical feedstocks: from mechanistic electrocatalysis models to system design. Adv Mater 2019;31:1807166. https://doi.org/10.1002/adma.201807166.

[7] Arshad F, Haq Tu, Hussain I, Sher F. Recent advances in electrocatalysts toward alcohol-assisted, energy-saving hydrogen production. ACS Appl Energy Mater 2021;4:8685–701. https://doi.org/10.1021/acsaem.1c01932.

[8] Zhang W, Yang Y, Huang B, Lv F, Wang K, Li N, et al. Ultrathin PtNiM (M = Rh, Os, and Ir) nanowires as efficient fuel oxidation electrocatalytic materials. Adv Mater 2019;31:1805833. https://doi.org/10.1002/adma.201805833.

[9] Yu J, He Q, Yang G, Zhou W, Shao Z, Ni M. Recent advances and prospective in Ruthenium-based materials for electrochemical water splitting. ACS Catal 2019;9:9973–10011. https://doi.org/10.1021/acscatal.9b02457.

[10] Kim J, Shih P-C, Qin Y, Al-Bardan Z, Sun C-J, Yang H. A porous pyrochlore $Y_2[Ru_{1.6}Y_{0.4}]O_{7-\delta}$ electrocatalyst for enhanced performance towards the oxygen evolution reaction in acidic media. Angew Chem Int Ed 2018;57:13877–81. https://doi.org/10.1002/anie.201808825.

[11] Ni J, Cheng Q, Liu S, Wang M, He Y, Qian T, et al. Deciphering electrolyte selection for electrochemical reduction of Carbon dioxide and Nitrogen to high-value-added chemicals. Adv Funct Mater 2023;33:2212483. https://doi.org/10.1002/adfm.202212483.

[12] Li L, Li X, Sun Y, Xie Y. Rational design of electrocatalytic carbon dioxide reduction for a zero-carbon network. Chem Soc Rev 2022;51:1234–52. https://doi.org/10.1039/D1CS00893E.

[13] Wang W, Lei B, Guo S. Engineering multimetallic nanocrystals for highly efficient oxygen reduction catalysts. Adv Energy Mater 2016;6:1600236. https://doi.org/10.1002/aenm.201600236.

[14] Feng J, Chen D, Pikhitsa PV, Jung Y-h, Yang J, Choi M. Unconventional alloys confined in nanoparticles: building blocks for new matter. Matter 2020;3:1646–63. https://doi.org/10.1016/j.matt.2020.07.027.

[15] Kasian O, Grote J-P, Geiger S, Cherevko S, Mayrhofer KJJ. The common intermediates of oxygen evolution and dissolution reactions during water electrolysis on Iridium. Angew Chem Int Ed 2018;57:2488–91. https://doi.org/10.1002/anie.201709652.

[16] Luo X, Liu C, Wang X, Shao Q, Pi Y, Zhu T, et al. Spin regulation on 2D Pd–Fe–Pt nanomeshes promotes fuel electrooxidations. Nano Lett 2020;20:1967–73. https://doi.org/10.1021/acs.nanolett.9b05250.

[17] Luo W-B, Pham TV, Guo H-P, Liu H-K, Dou S-X. Three-dimensional array of TiN@Pt_3Cu nanowires as an efficient porous electrode for the Lithium–Oxygen battery. ACS Nano 2017;11:1747–54. https://doi.org/10.1021/acsnano.6b07644.

[18] Amiri A, Shahbazian-Yassar R. Recent progress of high-entropy materials for energy storage and conversion. J Mater Chem A 2021;9:782–823. https://doi.org/10.1039/D0TA09578H.

[19] Liu H, Syama L, Zhang L, Lee C, Liu C, Dai Z, et al. High-entropy alloys and compounds for electrocatalytic energy conversion applications. SusMat 2021;1:482–505. https://doi.org/10.1002/sus2.32.

[20] Glasscott MW. Classifying and benchmarking high-entropy alloys and associated materials for electrocatalysis: a brief review of best practices. Curr Opin Electrochem 2022;34:100976. https://doi.org/10.1016/j.coelec.2022.100976.

[21] Du M, Li X, Pang H, Xu Q. Alloy electrocatalysts. EnergyChem 2023;5:100083. https://doi.org/10.1016/j.enchem.2022.100083.

[22] Yao Y, Liu Z, Xie P, Huang Z, Li T, Morris D, et al. Computationally aided, entropy-driven synthesis of highly efficient and durable multi-elemental alloy catalysts. Sci Adv 2020;6:eaaz0510. https://doi.org/10.1126/sciadv.aaz0510.

[23] Cherevko S, Geiger S, Kasian O, Kulyk N, Grote J-P, Savan A, et al. Oxygen and hydrogen evolution reactions on Ru, RuO_2, Ir, and IrO_2 thin film electrodes in acidic and alkaline electrolytes: a comparative study on activity and stability. Catal Today 2016;262:170–80. https://doi.org/10.1016/j.cattod.2015.08.014.

[24] Geiger S, Kasian O, Ledendecker M, Pizzutilo E, Mingers AM, Fu WT, et al. The stability number as a metric for electrocatalyst stability benchmarking. Nat Catal 2018;1:508–15. https://doi.org/10.1038/s41929-018-0085-6.

[25] Ron T, Shirizly A, Aghion E. Additive manufacturing technologies of high entropy alloys (HEA): review and prospects. Materials 2023;16:2454. https://www.mdpi.com/1996-1944/16/6/2454.

[26] Lu ZP, Wang H, Chen MW, Baker I, Yeh JW, Liu CT, et al. An assessment on the future development of high-entropy alloys: Summary from a recent workshop. Intermetallics 2015;66:67–76. https://doi.org/10.1016/j.intermet.2015.06.021.

[27] Zhang Y, Zuo TT, Tang Z, Gao MC, Dahmen KA, Liaw PK, et al. Microstructures and properties of high-entropy alloys. Prog Mater Sci 2014;61:1–93. https://doi.org/10.1016/j.pmatsci.2013.10.001.

[28] Jiang L, Lu Y, Dong Y, Wang T, Cao Z, Li T. Annealing effects on the microstructure and properties of bulk high-entropy $CoCrFeNiTi_{0.5}$ alloy casting ingot. Intermetallics 2014;44:37–43. https://doi.org/10.1016/j.intermet.2013.08.016.

[29] Salishchev GA, Tikhonovsky MA, Shaysultanov DG, Stepanov ND, Kuznetsov AV, Kolodiy IV, et al. Effect of Mn and V on structure and mechanical properties of high-entropy alloys based on CoCrFeNi system. J Alloys Compd 2014;591:11–21. https://doi.org/10.1016/j.jallcom.2013.12.210.

[30] Lei Z, Liu X, Wu Y, Wang H, Jiang S, Wang S, et al. Enhanced strength and ductility in a high-entropy alloy via ordered oxygen complexes. Nature 2018;563:546–50. https://doi.org/10.1038/s41586-018-0685-y.

[31] Yao Y, Huang Z, Xie P, Lacey SD, Jacob RJ, Xie H, et al. Carbothermal shock synthesis of high-entropy-alloy nanoparticles. Science 2018;359:1489–94. https://doi.org/10.1126/science.aan5412.

[32] Wang YP, Li BS, Fu HZ. Solid solution or intermetallics in a high-entropy alloy. Adv Eng Mater 2009;11:641–4. https://doi.org/10.1002/adem.200900057.

[33] Xiao DH, Zhou PF, Wu WQ, Diao HY, Gao MC, Song M, et al. Microstructure, mechanical and corrosion behaviors of AlCoCuFeNi-(Cr,Ti) high entropy alloys. Mater Des 2017;116:438–47. https://doi.org/10.1016/j.matdes.2016.12.036.

[34] Yeh JW. Recent progress in high-entropy alloys. Ann Chim Sci Mat 2006;31:633–48. https://doi.org/10.3166/acsm.31.633-648.

[35] Wu Z, Bei H, Otto F, Pharr GM, George EP. Recovery, recrystallization, grain growth and phase stability of a family of FCC-structured multi-component equiatomic solid solution alloys. Intermetallics 2014;46:131–40. https://doi.org/10.1016/j.intermet.2013.10.024.

[36] Daoud HM, Manzoni A, Völkl R, Wanderka N, Glatzel U. Microstructure and tensile behavior of $Al_8Co_{17}Cr_{17}Cu_8Fe_{17}Ni_{33}$ (at.%) high-entropy alloy. JOM 2013;65:1805–14. https://doi.org/10.1007/s11837-013-0756-3.

[37] Miracle DB, Senkov ON. A critical review of high entropy alloys and related concepts. Acta Mater 2017;122:448–511. https://doi.org/10.1016/j.actamat.2016.08.081.

[38] Tsai KY, Tsai MH, Yeh JW. Sluggish diffusion in Co–Cr–Fe–Mn–Ni high-entropy alloys. Acta Mater 2013;61:4887–97. https://doi.org/10.1016/j.actamat.2013.04.058.

[39] Yeh J-W, Chang S-Y, Hong Y-D, Chen S-K, Lin S-J. Anomalous decrease in X-ray diffraction intensities of Cu–Ni–Al–Co–Cr–Fe–Si alloy systems with multi-principal elements. Mater Chem Phys 2007;103:41–6. https://doi.org/10.1016/j.matchemphys.2007.01.003.

[40] Yeh J-W, Lin S-J, Chin T-S, Gan J-Y, Chen S-K, Shun T-T, et al. Formation of simple crystal structures in Cu-Co-Ni-Cr-Al-Fe-Ti-V alloys with multiprincipal metallic elements. Metall Mater Trans A 2004;35:2533–6. https://doi.org/10.1007/s11661-006-0234-4.

[41] Gong M, Wang D-Y, Chen C-C, Hwang B-J, Dai H. A mini review on Nickel-based electrocatalysts for alkaline hydrogen evolution reaction. Nano Res 2016;9:28–46. https://doi.org/10.1007/s12274-015-0965-x.
[42] Gao MY, Yang C, Zhang QB, Zeng JR, Li XT, Hua YX, et al. Electrochemical preparation of Ni-La alloy films from N-butyl-N-Methyl pyrrolidinium dicyanamide ionic liquid as electrocatalysts for hydrogen evolution reaction. J Electrochem Soc 2017;164:D778. https://doi.org/10.1149/2.1751712jes.
[43] Yeh J-W. Physical metallurgy of high-entropy alloys. JOM 2015;67:2254–61. https://doi.org/10.1007/s11837-015-1583-5.
[44] Gao MC, Yeh J-W, Liaw PK, Zhang Y. High-entropy alloys: fundamentals and applications. Switzerland: Springer; 2016.
[45] Cheng C-Y, Yang Y-C, Zhong Y, Chen Y-Y, Hsu T, Yeh J-W. Physical metallurgy of concentrated solid solutions from low-entropy to high-entropy alloys. Curr Opin Solid State Mater Sci 2017;21:299–311. https://doi.org/10.1016/j.cossms.2017.09.002.
[46] Hsu W-L, Tsai C-W, Yeh A-C, Yeh J-W. Clarifying the four core effects of high-entropy materials. Nat Rev Chem 2024;8:471–85. https://doi.org/10.1038/s41570-024-00602-5.
[47] Liu F, Shi C, Guo X, He Z, Pan L, Huang Z-F, et al. Rational design of better hydrogen evolution electrocatalysts for water splitting: a review. Adv Sci 2022;9:2200307. https://doi.org/10.1002/advs.202200307.
[48] Xu Y, Wang C, Huang Y, Fu J. Recent advances in electrocatalysts for neutral and large-current-density water electrolysis. Nano Energy 2021;80:105545. https://doi.org/10.1016/j.nanoen.2020.105545.
[49] Ren J-T, Wang Y-S, Chen L, Gao L-J, Tian W-W, Yuan Z-Y. Binary FeNi phosphides dispersed on N,P-doped carbon nanosheets for highly efficient overall water splitting and rechargeable Zn-air batteries. Chem Eng J 2020;389:124408. https://doi.org/10.1016/j.cej.2020.124408.
[50] Durst J, Siebel A, Simon C, Hasché F, Herranz J, Gasteiger HA. New insights into the electrochemical hydrogen oxidation and evolution reaction mechanism. Energy Environ Sci 2014;7:2255–60. https://doi.org/10.1039/C4EE00440J.
[51] Zhu J, Hu L, Zhao P, Lee LYS, Wong K-Y. Recent advances in electrocatalytic hydrogen evolution using nanoparticles. Chem Rev 2020;120:851–918. https://doi.org/10.1021/acs.chemrev.9b00248.
[52] Park H, Lee E, Lei M, Joo H, Coh S, Fokwa BPT. Canonic-like HER activity of $Cr_{1-x}Mo_xB_2$ solid solution: overpowering Pt/C at high current density. Adv Mater 2020;32:2000855. https://doi.org/10.1002/adma.202000855.
[53] Liu S, Shen Y, Zhang Y, Cui B, Xi S, Zhang J, et al. Extreme environmental thermal shock induced dislocation-rich Pt nanoparticles boosting hydrogen evolution reaction. Adv Mater 2022;34:2106973. https://doi.org/10.1002/adma.202106973.
[54] Rao CNR, Chhetri M. Borocarbonitrides as metal-free catalysts for the hydrogen evolution reaction. Adv Mater 2019;31:1803668. https://doi.org/10.1002/adma.201803668.
[55] Morales-Guio CG, Stern L-A, Hu X. Nanostructured hydrotreating catalysts for electrochemical hydrogen evolution. Chem Soc Rev 2014;43:6555–69. https://doi.org/10.1039/C3CS60468C.
[56] Lu Q, Hutchings GS, Yu W, Zhou Y, Forest RV, Tao R, et al. Highly porous non-precious bimetallic electrocatalysts for efficient hydrogen evolution. Nat Commun 2015;6:6567. https://doi.org/10.1038/ncomms7567.
[57] Li L, Wang P, Shao Q, Huang X. Metallic nanostructures with low dimensionality for electrochemical water splitting. Chem Soc Rev 2020;49:3072–106. https://doi.org/10.1039/D0CS00013B.
[58] Quaino P, Juarez F, Santos E, Schmickler W. Volcano plots in hydrogen electrocatalysis – uses and abuses. Beilstein J Nanotechnol 2014;5:846–54. https://doi.org/10.3762/bjnano.5.96.
[59] Wang X, Zheng Y, Sheng W, Xu ZJ, Jaroniec M, Qiao S-Z. Strategies for design of electrocatalysts for hydrogen evolution under alkaline conditions. Mater Today 2020;36:125–38. https://doi.org/10.1016/j.mattod.2019.12.003.
[60] Mahmood J, Li F, Jung S-M, Okyay MS, Ahmad I, Kim S-J, et al. An efficient and pH-universal Ruthenium-based catalyst for the hydrogen evolution reaction. Nat Nanotechnol 2017;12:441–6. https://doi.org/10.1038/nnano.2016.304.
[61] Dinh C-T, Jain A, de Arquer FPG, De Luna P, Li J, Wang N, et al. Multi-site electrocatalysts for hydrogen evolution in neutral media by destabilization of water molecules. Nat Energy 2019;4:107–14. https://doi.org/10.1038/s41560-018-0296-8.
[62] Subbaraman R, Tripkovic D, Chang K-C, Strmcnik D, Paulikas AP, Hirunsit P, et al. Trends in activity for the water electrolyser reactions on 3d M(Ni,Co,Fe,Mn) hydr(oxy)oxide catalysts. Nat Mater 2012;11:550–7. https://doi.org/10.1038/nmat3313.
[63] Subbaraman R, Tripkovic D, Strmcnik D, Chang K-C, Uchimura M, Paulikas AP, et al. Enhancing hydrogen evolution activity in water splitting by tailoring Li^+-Ni$(OH)_2$-Pt interfaces. Science 2011;334:1256–60. https://doi.org/10.1126/science.1211934.
[64] Strmcnik D, Lopes PP, Genorio B, Stamenkovic VR, Markovic NM. Design principles for hydrogen evolution reaction catalyst materials. Nano Energy 2016;29:29–36. https://doi.org/10.1016/j.nanoen.2016.04.017.
[65] Gao S, Hao S, Huang Z, Yuan Y, Han S, Lei L, et al. Synthesis of high-entropy alloy nanoparticles on supports by the fast moving bed pyrolysis. Nat Commun 2020;11:2016. https://doi.org/10.1038/s41467-020-15934-1.
[66] Feng G, Ning F, Song J, Shang H, Zhang K, Ding Z, et al. Sub-2 nm ultrasmall high-entropy alloy nanoparticles for extremely superior electrocatalytic hydrogen evolution. J Am Chem Soc 2021;143:17117–27. https://doi.org/10.1021/jacs.1c07643.
[67] Zhang D, Shi Y, Zhao H, Qi W, Chen X, Zhan T, et al. The facile oil-phase synthesis of a multi-site synergistic high-entropy alloy to promote the alkaline hydrogen evolution reaction. J Mater Chem A 2021;9:889–93. https://doi.org/10.1039/D0TA10574K.
[68] Hao J, Zhuang Z, Cao K, Gao G, Wang C, Lai F, et al. Unraveling the electronegativity-dominated intermediate adsorption on high-entropy alloy electrocatalysts. Nat Commun 2022;13:2662. https://doi.org/10.1038/s41467-022-30379-4.
[69] Zhu H, Sun S, Hao J, Zhuang Z, Zhang S, Wang T, et al. A high-entropy atomic environment converts inactive to active sites for electrocatalysis. Energy Environ Sci 2023;16:619–28. https://doi.org/10.1039/D2EE03185J.
[70] Yao R-Q, Zhou Y-T, Shi H, Wan W-B, Zhang Q-H, Gu L, et al. Nanoporous surface high-entropy alloys as highly efficient multisite electrocatalysts for nonacidic hydrogen evolution reaction. Adv Funct Mater 2021;31:2009613. https://doi.org/10.1002/adfm.202009613.
[71] Shi H, Sun X-Y, Zeng S-P, Liu Y, Han G-F, Wang T-H, et al. Nanoporous nonprecious high-entropy alloys as multisite electrocatalysts for ampere-level current-density hydrogen evolution. Small Struct 2023;4:2300042. https://doi.org/10.1002/sstr.202300042.
[72] Huang Z-F, Xi S, Song J, Dou S, Li X, Du Y, et al. Tuning of lattice oxygen reactivity and scaling relation to construct better oxygen evolution electrocatalyst. Nat Commun 2021;12:3992. https://doi.org/10.1038/s41467-021-24182-w.
[73] Saguì NA, Ström P, Edvinsson T, Bayrak Pehlivan İ. Nickel site modification by high-valence doping: effect of Tantalum impurities on the alkaline water electro-oxidation by NiO probed by operando Raman spectroscopy. ACS Catal 2022;12:6506–16. https://doi.org/10.1021/acscatal.2c00577.
[74] Yoo JS, Rong X, Liu Y, Kolpak AM. Role of lattice oxygen participation in understanding trends in the oxygen evolution reaction on Perovskites. ACS Catal 2018;8:4628–36. https://doi.org/10.1021/acscatal.8b00612.
[75] Zagalskaya A, Alexandrov V. Role of defects in the interplay between adsorbate evolving and lattice oxygen mechanisms of the oxygen evolution reaction in RuO_2 and IrO_2. ACS Catal 2020;10:3650–7. https://doi.org/10.1021/acscatal.9b05544.
[76] Zhang N, Chai Y. Lattice oxygen redox chemistry in solid-state electrocatalysts for water oxidation. Energy Environ Sci 2021;14:4647–71. https://doi.org/10.1039/D1EE01277K.
[77] Wang J, Gao Y, Kong H, Kim J, Choi S, Ciucci F, et al. Non-precious-metal catalysts for alkaline water electrolysis: operando characterizations, theoretical calculations, and recent advances. Chem Soc Rev 2020;49:9154–96. https://doi.org/10.1039/D0CS00575D.
[78] Zhang N, Feng X, Rao D, Deng X, Cai L, Qiu B, et al. Lattice oxygen activation enabled by high-valence metal sites for enhanced water oxidation. Nat Commun 2020;11:4066. https://doi.org/10.1038/s41467-020-17934-7.
[79] Abreu-Sepulveda MA, Dhital C, Huq A, Li L, Bridges CA, Paranthaman MP, et al. The influence of Fe substitution in Lanthanum Calcium Cobalt oxide on the oxygen evolution reaction in alkaline media. J Electrochem Soc 2016;163:F1124. https://doi.org/10.1149/2.1311609jes.
[80] Suen N-T, Hung S-F, Quan Q, Zhang N, Xu Y-J, Chen HM. Electrocatalysis for the oxygen evolution reaction: recent development and future perspectives. Chem Soc Rev 2017;46:337–65. https://doi.org/10.1039/C6CS00328A.
[81] Ren J-T, Chen L, Tian W-W, Song X-L, Kong Q-H, Wang H-Y, et al. Rational synthesis of core-shell-structured Nickel Sulfide-based nanostructures for efficient seawater electrolysis. Small 2023;19:2300194. https://doi.org/10.1002/smll.202300194.
[82] Xu H, Shan C, Wu X, Sun M, Huang B, Tang Y, et al. Fabrication of layered double hydroxide microcapsules mediated by Cerium doping in metal–organic frameworks for boosting water splitting. Energy Environ Sci 2020;13:2949–56. https://doi.org/10.1039/D0EE02113J.
[83] Hu P, Chen L, Deming CP, Kang X, Chen S. Nanoparticle-mediated intervalence charge transfer: core-size effects. Angew Chem Int Ed 2016;55:1455–9. https://doi.org/10.1002/anie.201508985.
[84] Du X, Huang J, Zhang J, Yan Y, Wu C, Hu Y, et al. Modulating electronic structures of inorganic nanomaterials for efficient electrocatalytic water splitting. Angew Chem Int Ed 2019;58:4484–502. https://doi.org/10.1002/anie.201810104.
[85] Sarkar A, Velasco L, Wang D, Wang Q, Talasila G, de Biasi L, et al. High entropy oxides for reversible energy storage. Nat Commun 2018;9:3400. https://doi.org/10.1038/s41467-018-05774-5.
[86] Wu Y, Zhao Y, Zhai P, Wang C, Gao J, Sun L, et al. Triggering lattice oxygen activation of single-atomic Mo sites anchored on Ni–Fe oxyhydroxides nanoarrays for electrochemical water oxidation. Adv Mater 2022;34:2202523. https://doi.org/10.1002/adma.202202523.
[87] Lyu F, Wang Q, Choi SM, Yin Y. Noble-metal-free electrocatalysts for oxygen evolution. Small 2019;15:1804201. https://doi.org/10.1002/smll.201804201.
[88] Song J, Wei C, Huang Z-F, Liu C, Zeng L, Wang X, et al. A review on fundamentals for designing oxygen evolution electrocatalysts. Chem Soc Rev 2020;49:2196–214. https://doi.org/10.1039/C9CS00607A.
[89] Wang B, Zhao K, Yu Z, Sun C, Wang Z, Feng N, et al. In situ structural evolution of the multi-site alloy electrocatalyst to manipulate the intermediate for enhanced water oxidation reaction. Energy Environ Sci 2020;13:2200–8. https://doi.org/10.1039/D0EE00755B.
[90] Ma P, Zhang S, Zhang M, Gu J, Zhang L, Sun Y, et al. Hydroxylated high-entropy alloy as highly efficient catalyst for electrochemical oxygen evolution reaction. Sci China Mater 2020;63:2613–9. https://doi.org/10.1007/s40843-020-1461-2.
[91] Shi Q, Zhu C, Du D, Lin Y. Robust noble metal-based electrocatalysts for oxygen evolution reaction. Chem Soc Rev 2019;48:3181–92. https://doi.org/10.1039/C8CS00671G.

[92] Zhang B, Zheng X, Voznyy O, Comin R, Bajdich M, García-Melchor M, et al. Homogeneously dispersed multimetal oxygen-evolving catalysts. Science 2016; 352:333–7. https://doi.org/10.1126/science.aaf1525.
[93] Shan J, Zheng Y, Shi B, Davey K, Qiao S-Z. Regulating electrocatalysts via surface and interface engineering for acidic water electrooxidation. ACS Energy Lett 2019;4:2719–30. https://doi.org/10.1021/acsenergylett.9b01758.
[94] Halck NB, Petrykin V, Krtil P, Rossmeisl J. Beyond the volcano limitations in electrocatalysis – oxygen evolution reaction. Phys Chem Chem Phys 2014;16: 13682–8. https://doi.org/10.1039/C4CP00571F.
[95] Lal MS, Sundara R. High entropy oxides—a cost-effective catalyst for the growth of high yield carbon nanotubes and their energy applications. ACS Appl Mater Interfaces 2019;11:30846–57. https://doi.org/10.1021/acsami.9b08794.
[96] Liu Y, Chen G, Ge R, Pei K, Song C, Li W, et al. Construction of CoNiFe trimetallic carbonate hydroxide hierarchical hollow microflowers with oxygen vacancies for electrocatalytic water oxidation. Adv Funct Mater 2022;32:2200726. https://doi.org/10.1002/adfm.202200726.
[97] Liu D, Ai H, Li J, Fang M, Chen M, Liu D, et al. Surface reconstruction and phase transition on Vanadium–Cobalt–Iron trimetal nitrides to form active oxyhydroxide for enhanced electrocatalytic water oxidation. Adv Energy Mater 2020;10:2002464. https://doi.org/10.1002/aenm.202002464.
[98] Jin Z, Lv J, Jia H, Liu W, Li H, Chen Z, et al. Nanoporous Al-Ni-Co-Ir-Mo high-entropy alloy for record-high water splitting activity in acidic environments. Small 2019;15:1904180. https://doi.org/10.1002/smll.201904180.
[99] Li L, Wang P, Shao Q, Huang X. Recent progress in advanced electrocatalyst design for acidic oxygen evolution reaction. Adv Mater 2021;33:2004243. https://doi.org/10.1002/adma.202004243.
[100] Zhu H, Zhu Z, Hao J, Sun S, Lu S, Wang C, et al. High-entropy alloy stabilized active Ir for highly efficient acidic oxygen evolution. Chem Eng J 2022;431: 133251. https://doi.org/10.1016/j.cej.2021.133251.
[101] Huang K, Xia J, Lu Y, Zhang B, Shi W, Cao X, et al. Self-reconstructed spinel surface structure enabling the long-term stable hydrogen evolution reaction/ oxygen evolution reaction efficiency of FeCoNiRu high-entropy alloyed electrocatalyst. Adv Sci 2023;10:2300094. https://doi.org/10.1002/advs.202300094.
[102] Shao Q, Wang P, Huang X. Opportunities and challenges of interface engineering in bimetallic nanostructure for enhanced electrocatalysis. Adv Funct Mater 2019; 29:1806419. https://doi.org/10.1002/adfm.201806419.
[103] Anantharaj S, Aravindan V. Developments and perspectives in 3d transition-metal-based electrocatalysts for neutral and near-neutral water electrolysis. Adv Energy Mater 2020;10:1902666. https://doi.org/10.1002/aenm.201902666.
[104] Qiu H-J, Fang G, Gao J, Wen Y, Lv J, Li H, et al. Noble metal-free nanoporous high-entropy alloys as highly efficient electrocatalysts for oxygen evolution reaction. ACS Mater Lett 2019;1:526–33. https://doi.org/10.1021/acsmaterialslett.9b00414.
[105] Gao R, Yan D. Recent development of Ni/Fe-based micro/nanostructures toward photo/electrochemical water oxidation. Adv Energy Mater 2020;10:1900954. https://doi.org/10.1002/aenm.201900954.
[106] Huang K, Zhang B, Wu J, Zhang T, Peng D, Cao X, et al. Exploring the impact of atomic lattice deformation on oxygen evolution reactions based on a sub-5 nm pure face-centred cubic high-entropy alloy electrocatalyst. J Mater Chem A 2020; 8:11938–47. https://doi.org/10.1039/D0TA02125C.
[107] Cui X, Zhang B, Zeng C, Guo S. Electrocatalytic activity of high-entropy alloys toward oxygen evolution reaction. MRS Commun 2018;8:1230–5. https://doi.org/10.1557/mrc.2018.111.
[108] Li Y, Du X, Huang J, Wu C, Sun Y, Zou G, et al. Recent progress on surface reconstruction of earth-abundant electrocatalysts for water oxidation. Small 2019;15:1901980. https://doi.org/10.1002/smll.201901980.
[109] Chen J, Ling Y, Yu X, Wang G, Huang L, He A, et al. Water oxidation on CrMnFeCoNi high entropy alloy: improvement through rejuvenation and spin polarization. J Alloys Compd 2022;929:167344. https://doi.org/10.1016/j.jallcom.2022.167344.
[110] Broge NLN, Bertelsen AD, Søndergaard-Pedersen F, Iversen BB. Facile solvothermal synthesis of Pt–Ir–Pd–Rh–Ru–Cu–Ni–Co high-entropy alloy nanoparticles. Chem Mater 2023;35:144–53. https://doi.org/10.1021/acs.chemmater.2c02842.
[111] Wu D, Kusada K, Nanba Y, Koyama M, Yamamoto T, Toriyama T, et al. Noble-metal high-entropy-alloy nanoparticles: atomic-level insight into the electronic structure. J Am Chem Soc 2022;144:3365–9. https://doi.org/10.1021/jacs.1c13616.
[112] Fu X, Zhang J, Zhan S, Xia F, Wang C, Ma D, et al. High-entropy alloy nanosheets for fine-tuning hydrogen evolution. ACS Catal 2022;12:11955–9. https://doi.org/10.1021/acscatal.2c02778.
[113] Zhang G, Ming K, Kang J, Huang Q, Zhang Z, Zheng X, et al. High entropy alloy as a highly active and stable electrocatalyst for hydrogen evolution reaction. Electrochim Acta 2018;279:19–23. https://doi.org/10.1016/j.electacta.2018.05.035.
[114] Liu G, Song C, Li X, Jia Q, Wu P, Lou Z, et al. Defect-rich FeCoNiMnRu high-entropy alloys with activated interfacial water for boosting alkaline water/ seawater hydrogen evolution. Chem Eng J 2025;509:161070. https://doi.org/10.1016/j.cej.2025.161070.
[115] Zhang Y, Li Z, Jang H, Kim MG, Cho J, Liu S, et al. In situ grown RuNi alloy on $ZrNi_x$ as a bifunctional electrocatalyst boosts industrial water splitting. Adv Mater 2025:2501586. https://doi.org/10.1002/adma.202501586. n/a.
[116] Zhu A, Qiao L, Liu K, Gan G, Luan C, Lin D, et al. Rational design of precatalysts and controlled evolution of catalyst-electrolyte interface for efficient hydrogen production. Nat Commun 2025;16:1880. https://doi.org/10.1038/s41467-025-57056-6.
[117] Lai D, Kang Q, Gao F, Lu Q. High-entropy effect of a metal phosphide on enhanced overall water splitting performance. J Mater Chem A 2021;9:17913–22. https://doi.org/10.1039/D1TA04755H.
[118] Niu S, Yang Z, Qi F, Han Y, Shi Z, Qiu Q, et al. Electrical discharge induced bulk-to-nanoparticle transformation: nano high-entropy carbide as catalysts for hydrogen evolution reaction. Adv Funct Mater 2022;32:2203787. https://doi.org/10.1002/adfm.202203787.
[119] Liao S, Huang T, Wu W, Yang T, Hou Q, Sang S, et al. Engineering high-entropy duel-functional nanocatalysts with regulative oxygen vacancies for efficient overall water splitting. Chem Eng J 2023;471:144506. https://doi.org/10.1016/j.cej.2023.144506.
[120] Lei Y, Zhang L, Xu W, Xiong C, Chen W, Xiang X, et al. Carbon-supported high-entropy Co-Zn-Cd-Cu-Mn sulfide nanoarrays promise high-performance overall water splitting. Nano Res 2022;15:6054–61. https://doi.org/10.1007/s12274-022-4304-8.
[121] Chang S-Q, Cheng C-C, Cheng P-Y, Huang C-L, Lu S-Y. Pulse electrodeposited FeCoNiMnW high entropy alloys as efficient and stable bifunctional electrocatalysts for acidic water splitting. Chem Eng J 2022;446:137452. https://doi.org/10.1016/j.cej.2022.137452.
[122] Li S-Y, Nguyen TX, Su Y-H, Lin C-C, Huang Y-J, Shen Y-H, et al. Sputter-deposited high entropy alloy thin film electrocatalyst for enhanced oxygen evolution reaction performance. Small 2022;18:2106127. https://doi.org/10.1002/smll.202106127.
[123] Tang J, Xu JL, Ye ZG, Li XB, Luo JM. Microwave sintered porous CoCrFeNiMo high entropy alloy as an efficient electrocatalyst for alkaline oxygen evolution reaction. J Mater Sci Technol 2021;79:171–7. https://doi.org/10.1016/j.jmst.2020.10.079.
[124] Sharma L, Katiyar NK, Parui A, Das R, Kumar R, Tiwary CS, et al. Low-cost high entropy alloy (HEA) for high-efficiency oxygen evolution reaction (OER). Nano Res 2022;15:4799–806. https://doi.org/10.1007/s12274-021-3802-4.
[125] Hegde C, Lim CHJ, Teng TH, Liu D, Kim Y-J, Yan Q, et al. In situ synthesis and microfabrication of high entropy alloy and oxide compounds by femtosecond laser direct writing under ambient conditions. Small 2022;18:2203126. https://doi.org/10.1002/smll.202203126.
[126] Mei Y, Chen J, Wang Q, Guo Y, Liu H, Shi W, et al. MoZn-based high entropy alloy catalysts enabled dual activation and stabilization in alkaline oxygen evolution. Sci Adv 2024;10:eadq6758. https://doi.org/10.1126/sciadv.adq6758.
[127] Xia L, Gomes BF, Jiang W, Escalera-López D, Wang Y, Hu Y, et al. Operando-informed precatalyst programming towards reliable high-current-density electrolysis. Nat Mater 2025. https://doi.org/10.1038/s41563-025-02128-7.
[128] Huang Y, Wang Z, Xiao H, Liu Q, Wang X. Activating and stabilizing lattice oxygen via self-adaptive Zn–NiOOH sub-nanowires for oxygen evolution reaction. J Am Chem Soc 2024;146:29006–16. https://doi.org/10.1021/jacs.4c09931.
[129] Meyer TE, Peng CC, Lin C-Y, Ugras TJ, Shi Z, Zhao A, et al. Colloidal synthesis of thiospinel high-entropy sulfide star-like nanocrystals with high cycling stability for the oxygen evolution reaction. Nano Lett 2025;25:4234–41. https://doi.org/10.1021/acs.nanolett.4c05699.
[130] Sukkurji PA, Cui Y, Lee S, Wang K, Azmi R, Sarkar A, et al. Mechanochemical synthesis of novel rutile-type high entropy fluorides for electrocatalysis. J Mater Chem A 2021;9:8998–9009. https://doi.org/10.1039/D0TA10209A.
[131] Sun W, Wang Y, Liu S, Lei F, Xie J, Tang B. High-entropy amorphous oxycyanide as an efficient pre-catalyst for the oxygen evolution reaction. Chem Commun 2022;58:11981–4. https://doi.org/10.1039/D2CC04646F.
[132] Zhang J, Shi L, Miao X, Yang L, Zhou S. A new-type high-entropy electrocatalyst with a pyrochlore structure for acid-water oxidation. J Mater Chem A 2024;12: 12785–94. https://doi.org/10.1039/D4TA01382D.
[133] Gong S, Meng Y, Jin Z, Hsu H-Y, Du M, Liu F. Recent progress on the stability of electrocatalysts under high current densities toward industrial water splitting. ACS Catal 2024;14:14399–435. https://doi.org/10.1021/acscatal.4c03700.
[134] Chen F-Y, Wu Z-Y, Adler Z, Wang H. Stability challenges of electrocatalytic oxygen evolution reaction: from mechanistic understanding to reactor design. Joule 2021;5:1704–31. https://doi.org/10.1016/j.joule.2021.05.005.
[135] Sun M, Zhai Y, Wang J. Enhancing long-term stability in oxygen evolution through in-situ etching of phase segregation Fe-Mn oxide. Appl Catal B Environ 2024;358:124453. https://doi.org/10.1016/j.apcatb.2024.124453.
[136] Kuai C, Xu Z, Xi C, Hu A, Yang Z, Zhang Y, et al. Phase segregation reversibility in mixed-metal hydroxide water oxidation catalysts. Nat Catal 2020;3:743–53. https://doi.org/10.1038/s41929-020-0496-z.
[137] Kempler PA, Coridan RH, Luo L. Gas evolution in water electrolysis. Chem Rev 2024;124:10964–1007. https://doi.org/10.1021/acs.chemrev.4c00211.
[138] Prajapati A, Hahn C, Weidinger IM, Shi Y, Lee Y, Alexandrova AN, et al. Best practices for in-situ and operando techniques within electrocatalytic systems. Nat Commun 2025;16:2593. https://doi.org/10.1038/s41467-025-57563-6.
[139] Li S, Yan J, Chen X, Ni C, Chen Y, Liu M, et al. Advanced in situ characterization techniques for studying the dynamics of solid-liquid interface in electrocatalytic reactions. Mater Today Catal 2024;7:100068. https://doi.org/10.1016/j.mtcata.2024.100068.
[140] Dash S, K AS, S J, D VHW, D E, Surapraraju SK, et al. Advances in green hydrogen production through alkaline water electrolysis: a comprehensive review. Int J Hydrogen Energy 2024;83:614–29. https://doi.org/10.1016/j.ijhydene.2024.08.157.
[141] Domalanta MR, Bamba JN, Matienzo DJD, del Rosario-Paraggua JA, Ocon J. Pathways towards achieving high current density water electrolysis: from

material perspective to system configuration. ChemSusChem 2023;16:e202300310. https://doi.org/10.1002/cssc.202300310.
[142] Wei Z, Guo M, Zhang Q. Scalable electrodeposition of NiFe-based electrocatalysts with self-evolving multi-vacancies for high-performance industrial water electrolysis. Appl Catal B Environ 2023;322:122101. https://doi.org/10.1016/j.apcatb.2022.122101.
[143] Bolar S, Ito Y, Fujita T. Future prospects of high-entropy alloys as next-generation industrial electrode materials. Chem Sci 2024;15:8664–722. https://doi.org/10.1039/D3SC06784J.
[144] Li Y, Sun Y, Qin Y, Zhang W, Wang L, Luo M, et al. Recent advances on water-splitting electrocatalysis mediated by noble-metal-based nanostructured materials. Adv Energy Mater 2020;10:1903120. https://doi.org/10.1002/aenm.201903120.
[145] Xu Z, Wu Z-S. Scalable production of high-performance electrocatalysts for electrochemical water splitting at large current densities. eScience 2024:100334. https://doi.org/10.1016/j.esci.2024.100334.
[146] Li S, Li E, An X, Hao X, Jiang Z, Guan G. Transition metal-based catalysts for electrochemical water splitting at high current density: current status and perspectives. Nanoscale 2021;13:12788–817. https://doi.org/10.1039/D1NR02592A.
[147] Li H, Han Y, Zhao H, Qi W, Zhang D, Yu Y, et al. Fast site-to-site electron transfer of high-entropy alloy nanocatalyst driving redox electrocatalysis. Nat Commun 2020;11:5437. https://doi.org/10.1038/s41467-020-19277-9.
[148] Batchelor TAA, Pedersen JK, Winther SH, Castelli IE, Jacobsen KW, Rossmeisl J. High-entropy alloys as a discovery platform for electrocatalysis. Joule 2019;3:834–45. https://doi.org/10.1016/j.joule.2018.12.015.
[149] Bhattacharjee S, Waghmare UV, Lee S-C. An improved d-band model of the catalytic activity of magnetic transition metal surfaces. Sci Rep 2016;6:35916. https://doi.org/10.1038/srep35916.
[150] Kim D, Chung M, Kim S, Yun K, Cha W, Harder R, et al. Defect dynamics at a single Pt nanoparticle during catalytic oxidation. Nano Lett 2019;19:5044–52. https://doi.org/10.1021/acs.nanolett.9b01332.
[151] Shen J, Hu Z, Chen K, Chen C, Zhu Y, Li C. Platinum based high entropy alloy oxygen reduction electrocatalysts for proton exchange membrane fuel cells. Mater Today Nano 2023;21:100282. https://doi.org/10.1016/j.mtnano.2022.100282.
[152] Li S, Tang X, Jia H, Li H, Xie G, Liu X, et al. Nanoporous high-entropy alloys with low Pt loadings for high-performance electrochemical oxygen reduction. J Catal 2020;383:164–71. https://doi.org/10.1016/j.jcat.2020.01.024.
[153] Paul R, Zhu L, Chen H, Qu J, Dai L. Recent advances in Carbon-based metal-free electrocatalysts. Adv Mater 2019;31:1806403. https://doi.org/10.1002/adma.201806403.
[154] Xu Y, Li J, Chen W, Zhou J, He S, Zhu C, et al. Rapid synthesis of an OER catalytic surface on dual-phase high-entropy alloys via a controllable single-phase corrosion approach. Int J Hydrogen Energy 2024;61:1187–98. https://doi.org/10.1016/j.ijhydene.2024.02.344.
[155] He Y, Qin J, Hu F, Mao L, Shen B, Aminabhavi TM, et al. Chemical dealloying derived nanoporous FeCoNiCuTi high-entropy bifunctional electrocatalysts for highly efficient overall water splitting under alkaline conditions. Chem Eng J 2024;492:152145. https://doi.org/10.1016/j.cej.2024.152145.
[156] Wan W, Liang K, Zhu P, He P, Zhang S. Recent advances in the synthesis and fabrication methods of high-entropy alloy nanoparticles. J Mater Sci Technol 2024;178:226–46. https://doi.org/10.1016/j.jmst.2023.08.051.
[157] Ilcheva V, Boev V, Lefterova E, Avdeev G, Dimitrov O, Bojanova N, et al. Effect of gadolinium doping on the structure of $Ce_{1-x}Gd_xO_{2-x/2}$ solid solutions prepared by ionic gelation approach. Emerg Sci J 2024;8:1686–96. https://doi.org/10.28991/ESJ-2024-08-05-01.
[158] Shi W, Liu H, Zhang J, Shen S, Wang Y, Guo Y, et al. Roll-to-roll synthesis of multielement heterostructured catalysts. Nat Synth 2025. https://doi.org/10.1038/s44160-025-00758-y.
[159] Zhang W, Wei X, Wu T, Wei F, Ma L, Lv Y, et al. Carbothermal shock enabled functional nanomaterials for energy-related applications. Nano Energy 2023;118:108994. https://doi.org/10.1016/j.nanoen.2023.108994.
[160] Liu J, Wang X, Zong X, Ding X, Xu H, Yang F, et al. Superior strength-ductility synergy in novel as-cast $L1_2$-type HEI $Ni_{50}Co_{25}Cr_{9.5}Al_9Ti_5Ta_{1.5}$ with hierarchical core-shell structure. Acta Mater 2025;288:120811. https://doi.org/10.1016/j.actamat.2025.120811.
[161] Aziz S, Rehman NU, Soonmin H, Ahmad N. Novel Ni/ZnO nanocomposites for the effective photocatalytic degradation of malachite green dye. Civil Eng J 2024;10. https://doi.org/10.28991/CEJ-2024-010-08-011.
[162] Zhu L, Xue P, Lan Q, Meng G, Ren Y, Yang Z, et al. Recent research and development status of laser cladding: a review. Opt Laser Technol 2021;138:106915. https://doi.org/10.1016/j.optlastec.2021.106915.
[163] Zhang G, Ren Z, Hu J, Hou Y, Zheng H. Laser cladding-spraying fabrication of Al/Ni/WC@SMP-MoS_2 composite coating with enhanced anti-corrosion and self-lubricating property. Surf Coat Technol 2025;503:132017. https://doi.org/10.1016/j.surfcoat.2025.132017.
[164] Srivatsav VR, Ragunath S, Radhika N, Khan MA. Exploring the potential of gas atomized high entropy alloys in thermal spray coatings – a comprehensive review. J Mater Chem A 2024;12:29432–68. https://doi.org/10.1039/D4TA04512B.
[165] Lee C-C, Tasi IH, Chen S-H. Impact of phase separation on corrosion resistance of AlCrFeNi thermal spraying HEA coatings. Mater Chem Phys 2025:130757. https://doi.org/10.1016/j.matchemphys.2025.130757.
[166] Miao L, Jia W, Cao X, Jiao L. Computational chemistry for water-splitting electrocatalysis. Chem Soc Rev 2024;53:2771–807. https://doi.org/10.1039/D2CS01068B.
[167] Shan X, Pan Y, Cai F, Gao H, Xu J, Liu D, et al. Accelerating the discovery of efficient high-entropy alloy electrocatalysts: high-throughput experimentation and data-driven strategies. Nano Lett 2024;24:11632–40. https://doi.org/10.1021/acs.nanolett.4c03208.
[168] Kwon J, Sun S, Choi S, Lee K, Jo S, Park K, et al. Tailored electronic structure of Ir in high entropy alloy for highly active and durable bifunctional electrocatalyst for water splitting under an acidic environment. Adv Mater 2023;35:2300091. https://doi.org/10.1002/adma.202300091.
[169] Li Y, Tang J, Zhang H, Wang Y, Lin B, Qiao J, et al. In-situ construction and repair of high catalytic activity interface on corrosion-resistant high-entropy amorphous alloy electrode for hydrogen production in high-temperature dilute sulfuric acid electrolysis. Chem Eng J 2023;453:139905. https://doi.org/10.1016/j.cej.2022.139905.
[170] Pan Y, Shan X, Cai F, Gao H, Xu J, Zhou M. Accelerating the discovery of oxygen reduction electrocatalysts: high-throughput screening of element combinations in Pt-based high-entropy alloys. Angew Chem Int Ed 2024;63:e202407116. https://doi.org/10.1002/anie.202407116.
[171] Yao Y, Dong Q, Brozena A, Luo J, Miao J, Chi M, et al. High-entropy nanoparticles: synthesis-structure-property relationships and data-driven discovery. Science 2022;376:eabn3103. https://doi.org/10.1126/science.abn3103.
[172] Li H, Sun M, Pan Y, Xiong J, Du H, Yu Y, et al. The self-complementary effect through strong orbital coupling in ultrathin high-entropy alloy nanowires boosting pH-universal multifunctional electrocatalysis. Appl Catal B Environ 2022;312:121431. https://doi.org/10.1016/j.apcatb.2022.121431.
[173] Li H, Lai J, Li Z, Wang L. Multi-sites electrocatalysis in high-entropy alloys. Adv Funct Mater 2021;31:2106715. https://doi.org/10.1002/adfm.202106715.
[174] Wang Z, Zhang X, Wu X, Pan Y, Li H, Han Y, et al. High-entropy phosphate/C hybrid nanosheets for efficient acidic hydrogen evolution reaction. Chem Eng J 2022;437:135375. https://doi.org/10.1016/j.cej.2022.135375.
[175] Yu L, Zeng K, Li C, Lin X, Liu H, Shi W, et al. High-entropy alloy catalysts: from bulk to nano toward highly efficient carbon and nitrogen catalysis. Carbon Energy 2022;4:731–61. https://doi.org/10.1002/cey2.228.
[176] Cai H, Yang H, He S, Wan D, Kong Y, Li D, et al. Size-adjustable high-entropy alloy nanoparticles as an efficient platform for electrocatalysis. Angew Chem Int Ed 2024:e202423765. https://doi.org/10.1002/anie.202423765. n/a.
[177] Chen ZW, Li J, Ou P, Huang JE, Wen Z, Chen L, et al. Unusual Sabatier principle on high entropy alloy catalysts for hydrogen evolution reactions. Nat Commun 2024;15:359. https://doi.org/10.1038/s41467-023-44261-4.
[178] Gao H, Xu J, Zhang X, Zhou M. Benchmarking the intrinsic activity of transition metal oxides for the oxygen evolution reaction with advanced nanoelectrodes. Angew Chem Int Ed 2024;63:e202404663. https://doi.org/10.1002/anie.202404663.
[179] Hu Q, Wang H, Dai C, Lei X, Wang B, Liu X. Research advances in high-entropy alloy catalysts for water electrolysis under acidic conditions. J Electroanal Chem 2024;964:118313. https://doi.org/10.1016/j.jelechem.2024.118313.
[180] Tajuddin AAH, Wakisaka M, Ohto T, Yu Y, Fukushima H, Tanimoto H, et al. Corrosion-resistant and high-entropic non-noble-metal electrodes for oxygen evolution in acidic media. Adv Mater 2023;35:2207466. https://doi.org/10.1002/adma.202207466.
[181] Padama AAB, Palmero MA, Shimizu K, Chookajorn T, Watanabe S. Machine learning and density functional theory-based analysis of the surface reactivity of high entropy alloys: the case of H atom adsorption on CoCuFeMnNi. Comput Mater Sci 2025;247:113480. https://doi.org/10.1016/j.commatsci.2024.113480.
[182] Wang J, Xin S, Xiao Y, Zhang Z, Li Z, Zhang W, et al. Manipulating the water dissociation electrocatalytic sites of bimetallic Nickel-based alloys for highly efficient alkaline hydrogen evolution. Angew Chem Int Ed 2022;61:e202202518. https://doi.org/10.1002/anie.202202518.